Global Biogeochemical Cycles

RESEARCH ARTICLE
10.1029/2018GB006034

The Relationships Between Dissolved Zinc and Major Nutrients Phosphate and Silicate Along the GEOTRACES GA02 Transect in the West Atlantic Ocean

R. Middag[1], H. J. W. de Baar[1,2], and K. W. Bruland[3]

[1]Department of Ocean Systems (OCS), NIOZ Royal Netherlands Institute for Sea Research and Utrecht University, Texel, The Netherlands, [2]Department Ocean Ecosystems, University of Groningen, The Netherlands, [3]Department of Ocean Sciences and Institute of Marine Sciences, University of California Santa Cruz, Santa Cruz, CA, USA

Key Points:
- The West Atlantic distribution of dissolved Zn is dominated by advection and mixing rather than regional remineralization or scavenging
- Supply of nutrients to the surface ocean from underlying high-latitude water of both northern and southern origin is depleted in Zn
- Different water masses have different Zn-Si and Zn-PO_4 relations; there is no uniform linear Zn-nutrient relationship for the world oceans

Correspondence to:
R. Middag,
rob.middag@nioz.nl

Citation:
Middag, R., de Baar, H. J. W., & Bruland, K. W. (2019). The relationships between dissolved zinc and major nutrients phosphate and silicate along the GEOTRACES GA02 transect in the West Atlantic Ocean. *Global Biogeochemical Cycles*, *33*, 63–84. https://doi.org/10.1029/2018GB006034

Received 19 JUL 2018
Accepted 15 DEC 2018
Accepted article online 19 DEC 2018
Published online 24 JAN 2019

Abstract Dissolved zinc (Zn) has a nutrient-type distribution in the ocean that more closely resembles the distribution of silicate (Si) than phosphate (PO_4). However, Zn is a trace-nutrient and mostly present in the organic fraction of phytoplankton rather than the siliceous frustule. It has been suggested the coupling of Zn and Si is caused by the strong depletion of nutrients in the Southern Ocean, possibly combined with scavenging of Zn. Here we assess the distribution of Zn and nutrients along the conduit of southward traveling waters of northern origin and northward traveling waters of Antarctic origin to unravel the influence of various water masses and local biogeochemical processes in the Atlantic Ocean. The distribution of Zn and Si is governed by mixing such that influence of remineralization is barely distinguishable, whereas the distribution of PO_4 is influenced by both processes. The subsurface water masses that supply nutrients to the surface ocean are depleted in Zn. Indeed, the Southern Ocean water masses play a driving role, but remarkably, also subsurface water masses from northern high-latitude origin are depleted in Zn. Both northern and southern high-latitude waters have a relatively high Zn:PO_4 uptake and remineralization ratio, implying it is Zn availability and not only chronic iron limitation that leads to increased Zn uptake in the high-latitude regions. The limited supply of Zn to the surface Atlantic Ocean can explain the lack of an Atlantic Zn remineralization signal and indicates Zn might play a role in phytoplankton community composition and productivity.

1. Introduction

The low concentrations and complex matrix of seawater make sampling and analysis of trace metals challenging (Sohrin & Bruland, 2011). Consequently, there is a paucity in the amount of data and our understanding of the biogeochemical cycles of trace metals, including zinc (Zn; Little et al., 2016). Zn is an essential trace metal for phytoplankton growth, as it serves as a cofactor in several enzymes used in various processes such as the uptake of CO_2 and phosphorus (e.g., Morel et al., 1994, 2002; Shaked et al., 2006). The requirements for Zn by phytoplankton are lower than requirements for iron, but higher than for manganese and nickel (e.g., Bruland et al., 1991; de Baar et al., 2018; Twining & Baines, 2013). In the Earth's crust, Zn is a relatively minor constituent (70 ppm [mg/kg]; Taylor, 1964), but dissolved concentrations in seawater are at least 5 orders of magnitude lower with concentrations varying between <0.1 nmol/kg in surface waters to close to 12 nmol/kg at intermediate depths in the North Pacific (e.g., Bruland, 1980; Janssen & Cullen, 2015; Wyatt et al., 2014). Measurements of dissolved Zn in ocean waters are prone to contamination issues due to the presence of Zn in lab materials as well use as sacrificial anodes on equipment deployed in seawater. The first oceanographically consistent data for dissolved Zn in the ocean were produced around 1980 (Bruland, 1980; Bruland et al., 1979). These data showed that Zn had a nutrient type distribution in the ocean; that is, concentrations are depleted in the surface ocean due to uptake by phytoplankton, and concentrations increase with increasing depth due to remineralization (Bruland et al., 2014). However, in contrast to other metal nutrients such as Cd or Ni that closely resemble the distribution of the major nutrients nitrate (NO_3) and phosphate (PO_4), the distribution of Zn resembles the distribution of silicate (Si). This suggests that Zn is predominantly present within the diatom siliceous frustules or that Zn is associated with a refractory organic phase, both of which would regenerate more slowly in the water column (i.e., at greater depth) compared to NO_3 and PO_4 (e.g., Lohan et al., 2002;

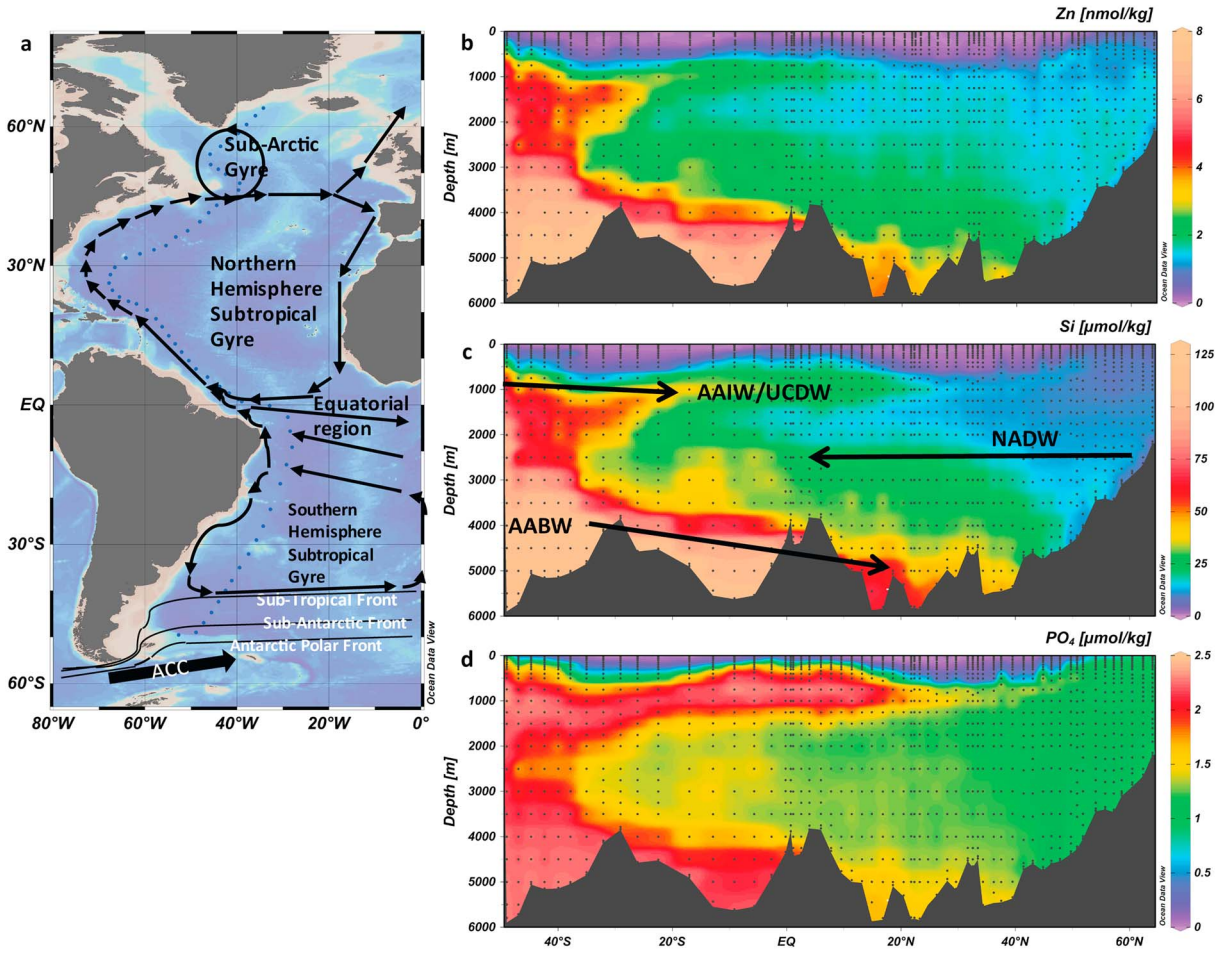

Figure 1. The 17,500-km-long GEOTRACES GA02 section in the West Atlantic Ocean. (a) The section is based on 4 cruises and comprising 60 stations (blue dots) with 24 sampling depths each and a general overview of the surface ocean circulation and key oceanographic features. (b) The concentration of dissolved Zn in color scale along the transect. (c) The concentration of dissolved Si in color scale along the transect. Abbreviations: AABW = Antarctic Bottom Water; NADW = North Atlantic Deep Water; AAIW = Antarctic Intermediate Water; UCDW = upper circumpolar deep water. (d) The concentration of dissolved PO_4 in color scale along the transect.

Zhao et al., 2014). However, it has been shown that only 1–3% of diatomaceous Zn is present within the siliceous frustules (Ellwood & Hunter, 2000a) and that most Zn is colocated with phosphorus in the organic tissue of diatoms and other phytoplankton (Twining et al., 2004a, 2004b). This would imply Zn should regenerate in a similar way as other nutrients and nutrient metals and have a distribution that more closely resembles NO_3 and PO_4. It has been suggested that the coupling between the Zn and Si distributions can be explained by scavenging; a fraction of Zn that was brought back into solution through regeneration is scavenged onto sinking, more refractory, particles. Despite the similar remineralization of Zn and PO_4, the scavenging of Zn but not PO_4 would give Zn a profile more similar to Si that remineralizes at greater depths (Conway & John, 2014; John & Conway, 2014). Alternatively, the coupling of Zn and Si might be coupled via strong depletion of both nutrients in the Southern Ocean (e.g., Ellwood, 2008; Saito et al., 2010; Sunda & Huntsman, 2000; Vance et al., 2017; Wyatt et al., 2014) or a combination of both scavenging and the strong depletion in the Southern Ocean (Weber et al., 2018).

Upwelling of deep water in the Southern Ocean supplies Si, Zn, PO_4, and NO_3 into surface waters, but during advection of the nutrient-rich surface water northward, Si and Zn get depleted much faster than PO_4 and NO_3. Notably at the Antarctic Polar Front (APF; Figure 1a) there is a steep decrease of Si and Zn (Lancelot et al., 2000, their Figure 5f; Klunder et al., 2011; their Figure 4.3; Zhao et al., 2014) in surface waters. This is attributed to intense blooms of large heavily silicified diatoms during austral spring and summer (Quéguiner et al., 1997). This means that in the formation regions at the APF and at the Sub-Antarctic

Front (SAF; Figure 1a) of Antarctic Intermediate Water (AAIW) and SubAntarctic Mode Water (SAMW), respectively, the Si and Zn are depleted with respect to NO_3 and PO_4. This AAIW and SAMW supply the lower latitude Atlantic Ocean with nutrients (Sarmiento et al., 2004), that is, a supply that is relatively depleted in Si and Zn versus PO_4 and NO_3. This would lead to similar distributions of Zn and Si at lower latitudes where the deep water is enriched in Si and Zn and the shallow surface waters are relatively depleted in Zn and Si.

The intensive circulation in the West Atlantic Ocean is one of the most pivotal components of the Great Ocean Conveyor (Broecker, 1991). This notion led us to design the 17,500-km-long GEOTRACES GA02 section of the Netherlands. The concentrations of Zn were measured along this West-Atlantic section in a campaign of four consecutive GEOTRACES cruises (2010–2012). This offers the opportunity to assess the distribution of Zn and nutrients along the conduit of the southward traveling deep North Atlantic Deep Water (NADW) and the northward traveling waters of Antarctic origin. The Zn measurements were all performed by the same analyst, and the shipboard PO_4 and Si measurements were done by members from the NIOZ nutrient laboratory that specializes in high-accuracy nutrient measurements. This generated a large internally consistent data set in which variations can be attributed to oceanic processes rather than analytical variability. The aim of this study is to elucidate the cycle of Zn in the West Atlantic and assess the role of the different water masses and local biogeochemical processes on the distribution of Zn in this convective basin. For such interpretations along this West Atlantic section, both Ocean Biogeochemical Cycling Modelling (Middag, Séférian, et al., 2015; van Hulten et al., 2013, 2014, 2017) and extended optimal multiple parameter (eOMP) analysis (Middag et al., 2018) have been applied. In general, each of both approaches provides much valuable insight, yet the outcome of the eOMP method is deemed to be more robust, as it requires much less adjustable parameters. Also, the eOMP method verifies directly versus the large data set of individual sample values without any further processing (e.g., averaging or binning) of the data set.

2. Materials and Methods

2.1. Sample Collection and Analysis

Samples were collected along the GEOTRACES GA02 Atlantic Meridional section of the Netherlands (Figure 1a) that consisted of four expeditions using the "Titan" ultraclean sampling system for trace metals (de Baar et al., 2008) with ultra-high purity grade Polyvinylidene Fluoride (PVDF) large volume samplers (Rijkenberg et al., 2015). A total of 60 full depth stations were occupied along the transect, each station comprising of 24 sampling depths; closing success of the samplers was 100%. After deployment, the complete CTD sampling system went into a clean room environment inside a modified high cube shipping container where subsamples were collected. The water for metal analysis was filtered from the PVDF samplers over a 0.2-μm filter cartridge (Sartobran-300, Sartorius) under pressure (0.5 bar overpressure) of (inline prefiltered) nitrogen gas, whereas the samples for nutrients were unfiltered. Subsamples for trace metal analysis were collected in acid-cleaned (following GEOTRACES protocol) low-density polyethylene sample bottles (500 ml) after five rinses with the sampled seawater. These seawater samples were acidified to a concentration of 0.024 M hydrochloric acid, which results in a pH of 1.7 to 1.8 with Baseline® hydrochloric acid (Seastar Chemicals Inc.). From these samples, a 40 ml subsample was taken for trace metal analysis using the multielement method as described previously (Biller & Bruland, 2012; Middag, van Hulten, et al., 2015). Briefly, this method uses Nobias-chelate PA1 resin to extract the metals from the seawater. After rinsing the resin with ultrapure water, the metals are eluted with nitric acid, and the extracts are run on a sector field inductively coupled plasma-mass spectrometer. The limit of detection was defined as the 3 times the standard deviation of the average blank along the entire transect and was 0.03 nmol/kg. Of the 1,433 values measured (for seven of the 1,440 samples, extraction failed and samples were not analyzed), 52 were rejected as outliers (see Middag et al., 2011, for criteria) and not used in the data set. Another 62 were below the limit of detection. These values were flagged but left in the data set. The absolute values are not used in any interpretation, but the data points were used in the plots where they represent the lowest range of the Zn distribution in the ocean. The results obtained at the BATS crossover station agree very well with data obtained by other analysts, and the results for the GEOTRACES and SAFe reference samples were in agreement with the consensus values (Middag, van Hulten, et al., 2015). Subsequently, the data were deemed intercalibrated by the GEOTRACES standards and intercalibration committee and are part of the GEOTRACES intermediate data product (Mawji et al., 2015; Schlitzer et al., 2018).

Samples for major nutrients (NO_3, nitrite [NO_2], PO_4, and Si [as Si $(OH)_4$]) were collected unfiltered from the PVDF samplers in high-density polyethylene sample bottles, which were rinsed three times with sample water. Nutrient concentrations were determined colorimetrically (Grasshoff et al., 1983) on a Bran en Luebbe trAAcs 800 Auto-analyzer. A sterilized natural reference nutrient sample (Kanso, Lot code AX) containing a known concentration of Si, PO_4, NO_3, and NO_2 in Pacific Ocean water was analyzed in triplicate every run. The precision of this reference sample was typically around 0.6% of the average value for Si, PO_4, and NO_3 and around 3% for NO_2. There was no significant difference between the shipboard measured values of Kanso and the consensus values (Rijkenberg et al., 2015). The detection limits were 0.01, 0.03, and 0.04 μmol/kg for PO_4, Si, and NO_3, respectively, with a precision of around 10% near the detection limit for PO_4 and around 3% for Si and NO_3. The deepest sample analyzed for a station of 24 samples was kept and reanalyzed within the next run of the next station of 24 samples as verification for variability between runs. The salinity (Conductivity), Temperature, and Depth (pressure) were measured with a CTD (Seabird SBE 911+). The CTD was calibrated before and after the expedition by the manufacturer (Seabird Electronics). Moreover, the conductivity sensors and oxygen sensors were calibrated against discrete water samples, analyzed on board.

2.2. Extended Optimum Multiparameter Analysis

The eOMP model used is the same as described by Middag et al. (2018). Briefly, contributions of seven predefined endmember water masses (composed of 11 water types; Tomczak, 1981) to each measured water sample were quantified using eOMP (based on 1,440 samples using potential temperature, salinity, NO_3, Si, and O_2; Mackas et al., 1987; Tomczak, 1981). The effects of remineralization were expressed as the deficit of oxygen, and this allows our analysis to be extended to include the nutrients and to be applied over large spatial scales (Karstensen & Tomczak, 1998; Middag et al., 2018, supporting information). This deficit of oxygen is O_2 mixing-O_2 observed, where O_2 mixing is the O_2 concentration one would expect based on conservative mixing of endmembers. The endmembers represent the extremes of this section and thus the calculated O_2 deficits only account for regional (i.e., within the Atlantic) remineralization.

3. Results and Discussion

3.1. Hydrographic Setting

The hydrography along the section has been described previously for this section (e.g., Middag, Séférian, et al., 2015; Rijkenberg et al., 2014). Briefly, North Atlantic Sub-Polar Mode Water (NASPMW) is found in the wind-driven Subarctic Gyre as surface water in the northernmost part of the transect (Figure 1a). Deep water formation that eventually results in NADW mainly takes place in the Labrador Sea and north of the Greenland-Scotland Ridge in the Greenland Sea and Arctic Ocean. Three components of NADW can be distinguished, Labrador Sea Water (LSW), Denmark Strait Overflow Water (DSOW), and Iceland-Scotland Overflow Water (ISOW; ISOW is not distinguished in the OMP; see Middag et al., 2018, for details). Around 45°N (near Grand Banks), there is the transition from the cold NASPMW into the warmer surface North Atlantic Sub-Tropical Mode Water (NASTMW) in the North Atlantic Sub-Tropical Gyre. Both NASPMW and NASTMW are considered components of the North Atlantic Central Water. In this region, NASTMW overlies the NASPMW (advected and subducted from the Subarctic Gyre), which in turn is underlain by NADW (between ~1,200 and 4,200 m). The deepest, near bottom, water mass was Antarctic Bottom Water (AABW), formed by deep water formation around Antarctica. In the North Atlantic it is also known as Lower Deep Water, because diapycnal mixing with overlying NADW modified this water mass. However, here it will be referred to as AABW to underline its Antarctic origin.

Further south, the near-equatorial region is characterized by a complex surface circulation with equatorial currents, countercurrents, and undercurrents (van Aken, 2007), not further discussed here. Fresher and less dense (compared to North Atlantic Central Water) Equatorial Surface Water was observed as far north as 26°N along the GEOTRACES GA02 transect. An Oxygen Minimum Zone was observed between ~20°N and ~15°S at depths between ~100 and 1,000 m. Additionally, three additional (sub-)Antarctic water masses, South Atlantic Sub-Polar Mode Water (SASPMW), AAIW, and upper Circumpolar Deep water (uCDW), can be distinguished. The SASPMW is also referred to more generally as Sub Antarctic Mode Water (SAMW), but as this water mass is also present in the Pacific and Indian Oceans, the name SASPMW will be used in this paper for the Atlantic variety. The SASPMW, AAIW, and uCDW advect northward at intermediate depth in

between the South Atlantic Sub-Tropical Mode Water (SASTMW) in the main thermocline of the South Atlantic subtropical gyre and the southward flowing NADW.

For PO_4 and NO_3, both the Antarctic origin intermediate-depth water masses and AABW are similarly elevated in nutrients with respect to the NADW, whereas Si is mainly elevated in AABW, but not so much in the intermediate-depth water masses of Antarctic origin (Figures 1c and 1d). The SASPMW can be distinguished just shallower than AAIW (Sarmiento et al., 2004), and SASTMW is found just below the seasonal thermocline (Provost et al., 1999). Both SASTMW and SASPMW can be considered precursors or source waters of South Atlantic Central Water (Stramma & England, 1999). Both SASPMW and AAIW are formed from Antarctic surface water. Around Antarctica, CDW upwells and subsequently advects northward. North of the Polar Front this surface water subducts as AAIW and continues to advect equatorward. North of the SAF, winter time mixing of Sub-Antarctic Surface Water with the underlying water creates the SASPMW that is dense enough to subduct, but less dense than the underlying AAIW. The SASPMW can be recognized by its high concentrations of NO_3 and PO_4 with respect to Si, expressed as Si* (Sarmiento et al., 2004) due to the faster depletion of Si compared to NO_3 and PO_4 during northward advection after upwelling of CDW. Given that AAIW is formed further south than SASPMW, the preferential depletion of Si with respect to NO_3 and PO_4 has a greater influence on SASPMW than on AAIW.

3.2. Basin Wide Distribution

The surface concentrations of dissolved Zn were depleted (<0.2 nmol/kg) in the surface layer along the entire transect with higher concentrations toward the northern end of the transect with values up to 0.9 nmol/kg (Figure 1b). Toward the southern end of the transect the surface concentrations remained low. Beyond the current transect, the surface Zn concentrations continue to increase northward up to ~4 nmol/kg (Danielsson & Westerlund, 1983; Moore, 1981) in the Arctic Ocean. In the Atlantic sector of the Southern Ocean, Zn concentrations also increase southward, with near surface concentrations up to ~3.7 nmol/kg south of the APF (Zhao et al., 2014), confirming the trend of increasing Zn concentrations toward the higher latitudes, a trend that exists in both the Northern Hemisphere (NH) and Southern Hemisphere (SH). Depleted surface concentrations persist to greater depths in the northern and southern subtropical gyres than at higher and lower latitudes. In the equatorial region this shoaling of the Zn isolines is probably the result of upwelling of deep water in combination with the presence of STMW in the gyres that was formed from low Zn surface waters. The inflow of relatively high Zn water in the north probably causes the shoaling of the isolines on the northern end. The generally depleted surface concentrations imply that any Zn input from external sources, such as atmospheric deposition or fluvial input, are either very small or rapidly depleted by biological uptake. As such external source for Zn cannot be identified from the current data set, they are considered to be negligible or only of localized importance as suggested previously (e.g., Kim et al., 2017; Wyatt et al., 2014).

In the entire West Atlantic Ocean, the concentrations of dissolved Zn increase with increasing depth, but this increase is much stronger in the SH due to the presence of relatively high Zn subsurface water masses from Antarctic origin; these are the AAIW, uCDW, and AABW. Notably, the AABW is enriched in Zn with concentrations up to 7.9 nmol/kg. This gives Zn a nutrient type distribution that resembles the distribution of Si more closely (Figures 1b and 1c) than the distribution of PO_4 (Figure 1d) or NO_3. The latter two are also elevated in the intermediate-depth Antarctic origin water masses (AAIW and uCDW) with concentrations of up to 100% of the maximum deep concentrations. In contrast, Zn and Si only show a comparatively modest increase in these water masses up to ~60% and 50%, respectively, of the maximum deep concentrations (Figure 1). The younger NADW from Nordic origin has comparatively low concentrations of nutrients and Zn, with increasing concentrations toward the south and the influence of the Antarctic origin water masses.

The DSOW has low Zn compared to the other two components of NADW, LSW and ISOW, akin to what was observed for cadmium (Cd; Middag et al., 2018). Given that this is also the case for the nutrients and the apparent oxygen utilization, less remineralization of organic matter in DSOW compared to LSW and ISOW is the most likely explanation, as ISOW and DSOW have a similar origin.

The very low Zn concentrations observed in the surface ocean and increasing concentrations with depth are consistent with previous observation in the South Atlantic (Wyatt et al., 2014) and North Atlantic (John &

Conway, 2014; Roshan & Wu, 2015). A similar distribution can be observed in the Pacific Ocean (e.g., Jakuba et al., 2012; Janssen & Cullen, 2015; Lohan et al., 2002), but with higher deep Zn concentrations as can be expected for a nutrient-type element (Bruland et al., 2014). The current section demonstrates for the first time that the depletion of Zn in surface waters occurs along the entire West Atlantic Ocean. Previously, it was suggested for the Sargasso Sea that PO_4 had to be depleted below 0.01 μmol/kg before Zn is depleted to values <0.2 nmol/kg (Jakuba et al., 2008), but the current data demonstrate that this is not necessarily the case elsewhere as such depleted Zn values were observed while PO_4 concentrations were as high as 1 μmol/kg.

In the following sections the distribution of Zn will be compared to the distribution of both PO_4 and Si. While generally the focus lies on the correlation between Zn and Si, we here also focus on the Zn-PO_4 relation to assess the hypothesis that the relative depletion of Zn and Si with respect to PO_4 in SAMW and AAIW is a driving factor in explaining the resemblance between the Zn and Si relationship.

3.3. Zn-PO_4 Relationship

In the following text section, the Zn-PO_4 relationship is systematically assessed from the northern end toward the southern end of the transect to identify the factors that influence the relationship. In this paper Zn/PO_4 (or Zn/Si) will be used to indicate a spot ratio (i.e., the dissolved ratio), Zn:PO_4 (or Zn:Si) to denote either a ratio of particles, and/or an uptake or remineralization ratio derived from a regression slope.

The progression southward is based on changes in the Zn-PO_4 relationship that are not obvious when assessing the data set as a whole. In the far north, north of 57.5°N, the Zn concentration is between 0.3 and 1.8 nmol/kg and reasonably well correlated with PO_4 (Figure 2a). The correlation is caused by LSW with relatively high concentrations of Zn and PO_4 that mixes with NASPMW, which in contrast has relatively low Zn and PO_4. Overall, this results in the shown correlation regression with a negative intercept (Figure. 2a). The DSOW has intermediate PO_4 concentrations with Zn levels higher than expected based on the LSW-NASPMW mixing line, resulting in scatter around the regression toward higher Zn concentrations (Figure 2a). Going southward till 50 °N, the relationship becomes distinctly bilinear with a so-called "kink" at a PO_4 concentration of ~0.9 μmol/kg (Figure 2b). This is caused by the mixing of low Zn (~0.1–0.8 nmol/kg) and relatively high PO_4 (~0.5–1 μmol/kg) NASPMW with underlying LSW with much higher Zn and only slightly higher PO_4 whereas the overlying surface water is depleted in both Zn and PO_4. In the deeper water column a similar three-water mass mixing distribution as north of 57.5°N is observed. Going southward (yet still north of 20°N), the bilinear relationship remains where data along the regression with the gentle slope (left of the kink) constitute mainly mixing between NASPMW and NASTMW where NASTMW has the lowest Zn and PO_4 concentrations and Zn is depleted (<0.2 nmol/kg) below a PO_4 concentration of 0.5 μmol/kg (Figure 2c). Data along the regression with the steep slope constitute mainly the deeper NADW (LSW and DSOW) mixing with NASPMW, as well as NADW mixing with AABW (slightly steeper slope). Around 750–1,000 m depth the deficit of oxygen (>75 μmol/kg) and PO_4 concentrations are elevated, resulting in data points that fall below the subsurface to deep (NASPMW-NADW-AABW) mixing line. This implies that regional remineralization adds Zn and PO_4 in a ratio that is not consistent with the deep water ratio but a ratio that is much lower (i.e., mainly contributes to PO_4 concentrations). The combined effect of remineralization and mixing with underlying water masses that are rich in both Zn and PO4 leads to the observed deviation of the bilinear relationship. Going toward the equator (Figure 2d), more data points are observed that are comparatively elevated in PO_4 and low in Zn. This constitutes intermediate water from Antarctic origin (SASPMW, AAIW, and uCDW mixture) with an appreciable deficit of oxygen (>75 μmol/kg), most likely due to interaction with the Oxygen Minimum Zone during advection. The mixing of these remineralization-influenced waters from Antarctic origin with remineralization-influenced water from Nordic origin results in the observed deviations from the bilinear relationship. Going further south, the same features remain in the Zn versus PO_4 distribution (Figure 3a) until relatively undiluted AAIW and uCDW without an appreciable oxygen deficit (<40 μmol/kg) appear, where AAIW has high PO_4 concentrations with relatively low Zn concentrations and uCDW that has both high PO_4 and high Zn concentrations (Figure 3b). However, the Zn concentrations in uCDW are lower than in AABW. Additionally, a clear kink becomes apparent in the NADW-AABW mixing line where the slope is steeper into relatively pure AABW. Thus, for the SH, the Zn versus PO_4 distribution is radically different from the

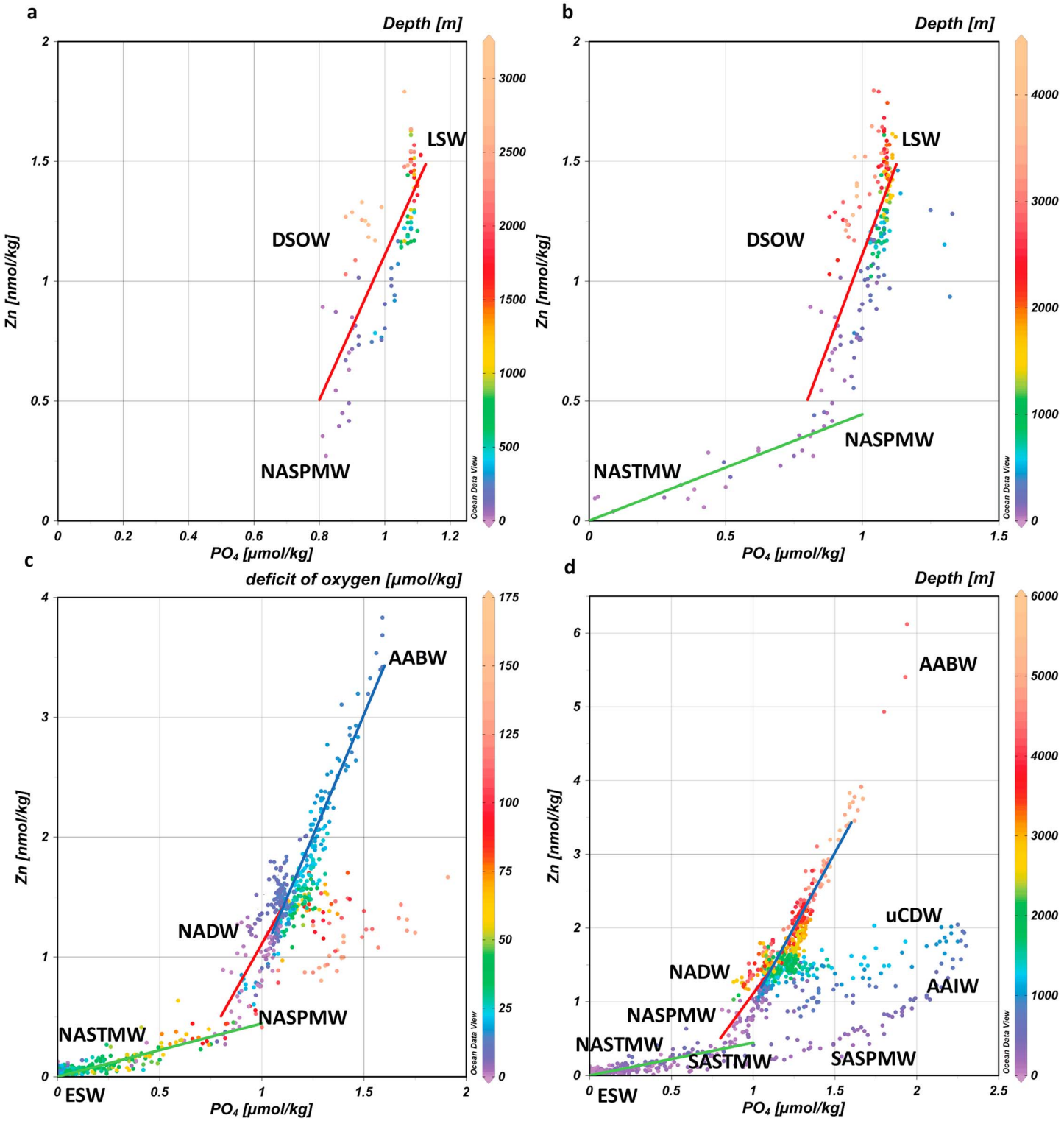

Figure 2. The Zn versus PO_4 distribution along the transect. (a) The distribution north of 57.5°N. (b) The distribution north of 50°N. (c) The distribution north of 20°N. (d) The distribution in the entire NH. Red line is the regression in Nordic water north of 57.5°N. Green line is the regression in surface water observed north of 50°N. Blue line is the regression observed in AABW north of 20N. Color scale indicates depth, except for Figure 2c where the deficit of oxygen is represented by the color scale. Equations for the regressions can be found in Table 2. Zn = zinc; LSW = Labrador Sea Water; DSOW = Denmark Strait Overflow Water; NASPMW = North Atlantic Sub-Polar Mode Water; NASTMW = North Atlantic Sub-Tropical Mode Water; AABW = Antarctic Bottom Water; NADW = North Atlantic Deep Water; uCDW = upper circumpolar deep water; AAIW = Antarctic Intermediate Water; SASPMW = South Atlantic Sub-Polar Mode Water; ESW = Equatorial Surface Water; NH = Northern Hemisphere.

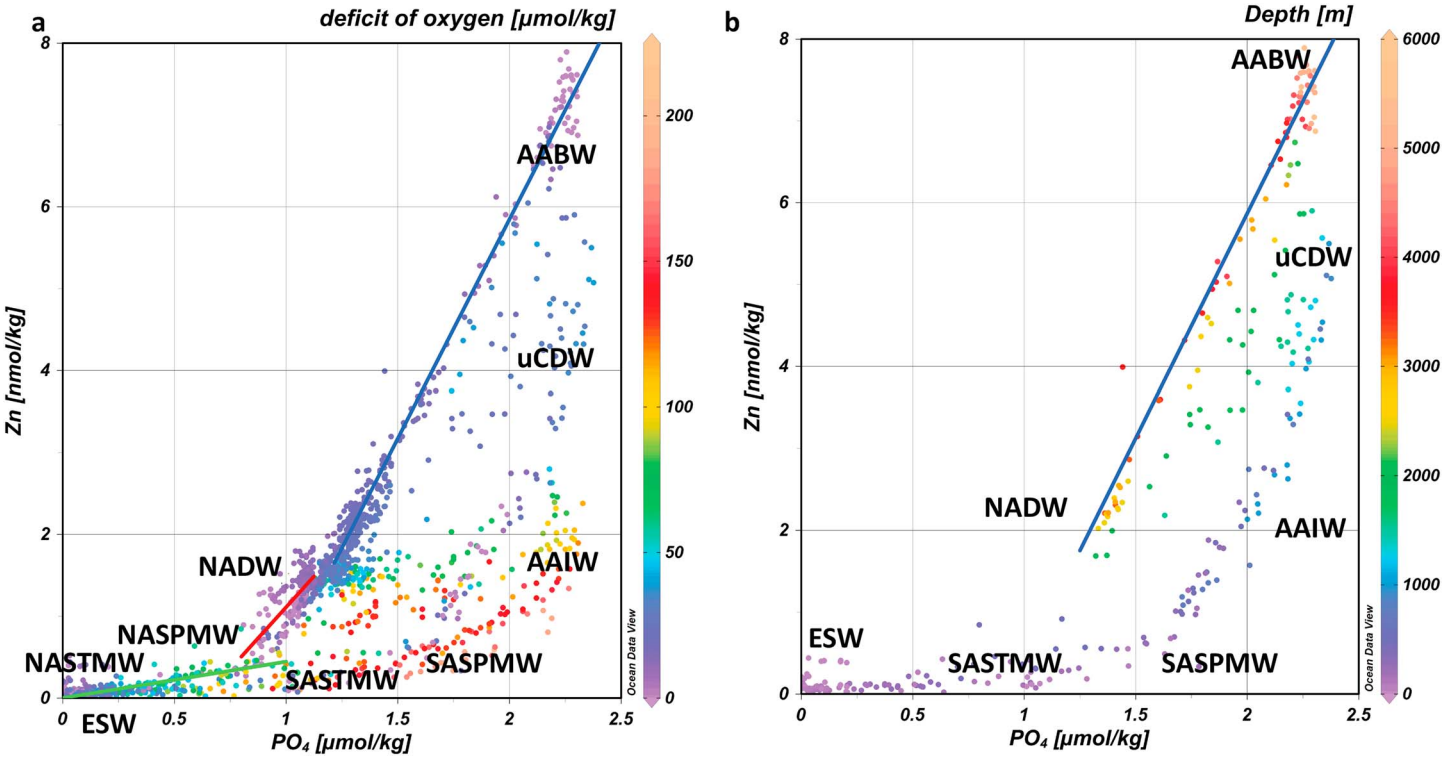

Figure 3. The Zn versus PO_4 distribution. (a) The distribution along the entire transect with the deficit of oxygen in color scale. (b) The distribution south of 20°S with depth in color scale. Red line is the regression in Nordic water north of 57.5°N. Green line is the regression in surface water observed north of 50°N. Blue line is the regression observed in AABW along the transect. Equations for the regressions can be found in Table 2. Zn = zinc; NASPMW = North Atlantic Sub-Polar Mode Water; NASTMW = North Atlantic Sub-Tropical Mode Water; AABW = Antarctic Bottom Water; NADW = North Atlantic Deep Water; uCDW = upper circumpolar deep water; AAIW = Antarctic Intermediate Water; ESW = Equatorial Surface Water; SASTMW = South Atlantic Sub-Tropical Mode Water; SASPMW = South Atlantic Sub-Polar Mode Water.

NH. In the NH there is the bilinear relationship with deviations caused by regional remineralization and mixing, notably with Antarctic origin water masses. Surface waters are depleted in both PO_4 and Zn in both hemispheres, notably at the lower latitudes. However, in the SH with increasing depth notably the PO_4 concentrations increase rapidly in SASPMW without a concurrent increase in Zn until the depth of AAIW and uCDW mixing. At greater depths in the SH, NADW is present with much lower PO_4 than in AAIW and uCDW, and Zn concentrations that are lower than in uCDW. However, Zn is in the same range (or even slightly higher) as observed in AAIW. Going from the surface to the deep ocean in the SH, this results in a complex Zn versus PO_4 distribution. In the surface and subsurface there is a Zn-PO_4 relationship with a very gentle positive slope until the Zn and PO_4 concentrations increase due to the influence of AAIW-uCDW mixing, and the relationship gets a steep slope. Going deeper, the relationship still has a steep slope, but the concentrations decrease with increasing depth due to mixing of uCDW and NADW. In the deepest part of the water column, there is yet again a relationship with a steep slope and concentrations that increase with increasing depth (NADW-AABW mixing), and additionally, there is a steepening of the slope into relatively undiluted AABW. Obviously, there is no general Zn-PO_4 relationship, and mixing plays a dominant role in the Zn-PO_4 distribution.

3.4. Comparison of the Zn-PO_4 and Cd-PO_4 Relationships

The overall Zn versus PO_4 distribution is very different from the Cd-PO_4 distribution. For the latter it was shown that the difference between the Antarctic origin and Nordic origin water masses leads to the well-known kink in this relationship (Middag et al., 2018). This in turn was related to different uptake and remineralization ratios in the source regions, where the regional remineralization ratio within the Atlantic was more comparable to the slope of the relationship in water masses of Nordic origin (NASPMW and NADW) than in water masses of southern origin (SASPMW, AAIW, uCDW, and AABW; Middag et al., 2018). Remineralization caused some deviations from the bilinear Cd-PO_4 relationship, as did the mixing

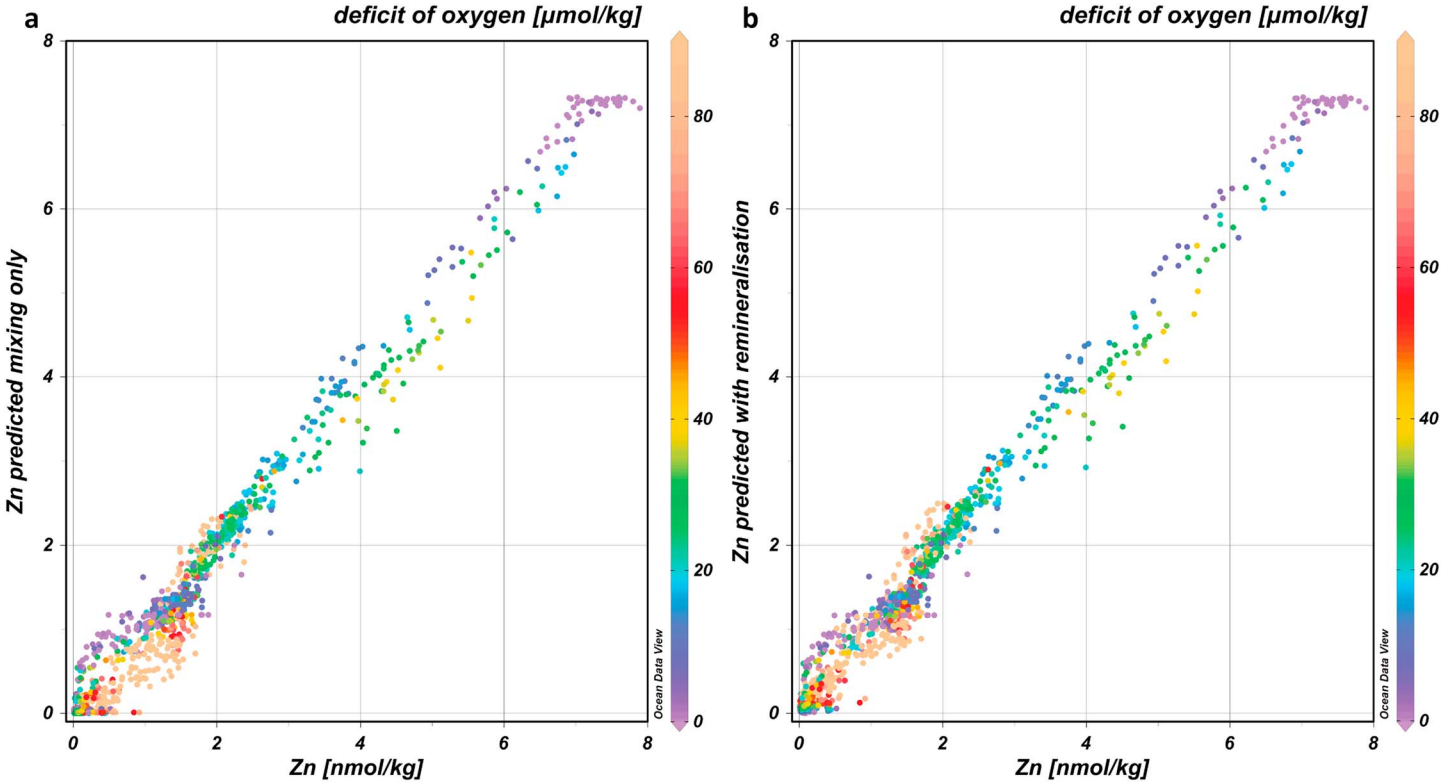

Figure 4. The eOMP model predicted Zn concentrations versus the observed Zn concentrations for 1,381 (1,433–52 outliers) individual samples. (a) A mixing-only model. (b) A model with both mixing and remineralization. The deficit of oxygen is indicated in color scale. The regression in Figure 4a can be described by Zn predicted = 0.99 * Zn observed – 0.06; R^2 = 0.98, RMSE = 0.23 nmol/kg. The regression in Figure 4b can be described by Zn predicted = 0.98 * Zn observed + 0.03; R^2 = 0.98, RMSE = 0.21 nmol/kg. Zn = zinc; eOMP = Optimal Multiple Parameter; RMSE = root mean square error.

between Antarctic origin subsurface water with Atlantic surface waters. For the Zn-PO_4 distribution, the relationship in NADW also has a different slope compared to the deep and intermediate-depth Antarctic origin water masses (Figures 2 and 3), implying different uptake and remineralization ratios for these water masses, akin to the Cd:PO_4 ratios. However, the Zn-PO_4 relationship in surface water masses formed in the Atlantic as well as SASPMW and NASPMW is radically different from the deeper lying water masses formed at the northern and southern higher latitudes. Mixing of these surface and subsurface water masses with underlying water masses, combined with the effects of regional remineralization in the Atlantic, causes large deviations in the Zn-PO_4 distribution that thus cannot be described by a single linear regression. There is a kink in the Zn-PO_4 relationship in NADW-AABW as observed in the Cd-PO_4 distribution, but in the overall Zn-PO_4 distribution this is a minor feature that is easily overlooked.

3.5. Remineralization and Mixing Using the eOMP Approach

Here we use the same eOMP model for this West Atlantic section as previously for Cd (Middag et al., 2018) that infers fractional contributions of various source water types to samples, based on the suite of five tracers (potential temperature, salinity, NO_3, Si, and O_2). Next the concentrations of Zn are predicted by straightforward multiplication of these fractions with assigned endmember Zn concentrations (estimated from our observations). The predicted Zn concentrations resemble the measured Zn concentrations well (R^2 = 0.97, root mean square error [RMSE] = 0.29 nmol/kg) when using a mixing only model. Subsequently, an optimized set of Zn endmember definitions was derived by inversion (see Middag et al., 2018, for details), which slightly improved the model fit (Figure 4a; R^2 = 0.98, RMSE = 0.23 nmol/kg), similar to what was observed for Cd. However, for Cd, the model fit could be markedly improved by accounting for the effect of remineralization. Contrarily, for Zn this barely improved the model fit (Figure 4b; R^2 = 0.98, RMSE = 0.21 nmol/kg), as the mixing only model already reproduces the Zn observations remarkably well along this meridional

Table 1
Predetermined and eOMP Endmember Solutions (Mixing Only and Mixing Plus Remineralization Model) for the Zn Concentration (nmol/kg) in the Various Water Types

Water type	Predetermined	Optimized mixing only	Optimized mixing and remineralization		
	Zn	Zn	Zn	Zn/Si	Zn/PO_4
AABW	8.00	7.69	7.67	0.06	3.32
DSOW	1.25	0.99	0.99	0.11	1.04
LSW	1.50	1.42	1.36	0.14	1.29
uCDW	4.50	5.16	5.01	0.08	2.11
AAIW	1.50	1.29	1.16	0.09	0.65
SASPMW	0.20	0.29	0.01	0.003	0.02
SASTMW	0.10	0.07	0.00	0.001	0.12
NASPMW	0.10	0.75	0.55	0.09	0.89
NASTMW	0.10	0.04	0.00	N/A	N/A
ESW-1	0.05	0.05	0.04	0.04	N/A
ESW-2	0.05	0.06	0.06	0.12	N/A

Note. Zn = zinc; Si = silicate; PO_4 = phosphate; AABW = Antarctic Bottom Water; DSOW = Denmark Strait Overflow Water; LSW = Labrador Sea Water; uCDW = upper Circumpolar Deep Water; AAIW = Antarctic Intermediate Water; SASPMW = South Atlantic Sub-Polar Mode Water; NASPMW = North Atlantic Sub-Polar Mode Water; NASTMW = North Atlantic Sub-Tropical Mode Water; ESW = Equatorial Surface Water. The dissolved Zn/Si and Zn/PO_4 ratio values (in units of nmol/μmol, i.e., 10^{-3} mol/mol) are based on the optimized Zn endmembers and the eOMP Si and PO_4 endmembers (see Middag et al., 2018, for details). For the optimized mixing and remineralization model, the remineralization ratio Zn:-O_2 (derived using the O_2 deficit) is 2.3×10^{-6} mol/mol. This Zn:− O_2 ratio can be converted to a $Zn:PO_4$ ratio using a $-O_2:PO_4$ ratio of 170:1 (0.40) and to a Zn:Si ratio using a $Si:PO_4$ ratio of 15:1 (0.027).

data set, similar to observations in the North Atlantic (Roshan & Wu, 2015) and consistent with the idea that different processes affect the Cd and Zn isotopic fraction in this region (John & Conway, 2014).

3.6. No Clear Remineralization or Scavenging Signal Distinguishable for Zn

The apparent lack of an influence of regional remineralization on the distribution of Zn is somewhat surprising, as remineralization causes deviations in the Zn-PO_4 relationship (see section 3.3). However, it can already be seen from the Zn-PO_4 plots that remineralization mainly affects the PO_4 concentrations and has a comparatively small effect on the Zn concentration and that mixing with deeper waters has a much stronger influence on the Zn concentration. In the case of Cd, a 1 μmol/kg increase in PO_4 due to remineralization would result in a ~0.2 nmol/kg increase in Cd, which is a quarter of the entire range of Cd concentrations observed in the West Atlantic (Middag et al., 2018). For Zn such remineralization would result in a ~0.6–2 nmol/kg (based on ratios by Ho et al., 2003; Twining et al., 2011) increase in the Zn concentration, which is merely one tenth to a quarter of the Zn range observed in the West Atlantic. The eOMP model infers a $Zn:PO_4$ regional remineralization ratio of 0.40 nmol/μmol for the West Atlantic (Table 1), implying an even smaller effect of remineralization on the Zn distribution. Additionally, unlike Cd and PO_4, part of remineralized Zn may be scavenged again as suggested previously (Conway & John, 2014; John & Conway, 2014), decreasing the net return of dissolved Zn into the water column. A recent world ocean simulation study (Weber et al., 2018) suggested that in addition to the role of Southern Ocean nutrient depletion and circulation, reversible scavenging of Zn onto organic particles would play a significant role in the Zn distribution, notably in the Pacific Ocean. Good quality data for the Southern Ocean endmember water masses that play a pivotal role in such simulations are scarce, with only a small data set from the Zero Meridian in the Atlantic sector of the Southern Ocean used (Zhao et al., 2014). Nevertheless, the incorporation of scavenging significantly improved the agreement between observations and model predictions, compared to a model without no scavenging, and can resolve the Zn isotopic mass balance in the ocean (Weber et al., 2018). Otherwise, Weber et al. (2018, supporting information) conclude that the Atlantic Ocean is rapidly ventilated by NADW from the north and southern ocean water masses from the south, so develops a much weaker accumulation (*due to remineralization and reversible scavenging*) signal of Zn without a clear vertical structure (indistinguishable from zero in most of the water column). This cited notion of Weber et al. (2018, supporting information) is in agreement with our independent findings (i.e., by very different eOMP approach based

on endmembers at the extremes of our section) that the Atlantic Ocean distribution of Zn is dominated by advection from high-latitude source waters.

As Zn is a required nutrient, obviously, there must be biological uptake and some remineralization, perhaps in combination with scavenging, but mixing is the dominant factor for the Zn distribution of the West Atlantic where any effect of regional remineralization or scavenging cannot be distinguished from mixing of radically different endmembers. Nevertheless, the stark contrast between the Zn-PO_4 composition of Atlantic surface waters compared to the deeper water masses with high latitude origin implies the uptake and remineralization of Zn with respect to PO_4 in the Atlantic is very different compared to the Antarctic and Nordic source regions of deep water. In the source regions of NADW, the Zn:PO_4 uptake and remineralization ratios are probably higher than in the Atlantic as evident from the relationship with a relatively steep slope in NADW (Figures 2 and 3), but data are currently lacking for the source regions of NADW. For the Antarctic source regions of deep water, the current observations are consistent with previous work in the Southern Ocean where Croot et al. (2011) reported slopes for the Zn-PO_4 relationship that increased from $<$2 nmol/μmol north of the polar front to values up to 7 nmol/μmol near the Antarctic continent in the upper water column. A similar trend and slope values were calculated based on the more recent Zn data by Zhao et al. (2014) and the corresponding PO_4 data (Schlitzer et al., 2018) and are in accordance with the estimated Southern Ocean uptake ratios calculated previously (Vance et al., 2017). This indeed indicates the Zn:PO_4 uptake and remineralization ratios are higher in the source regions of Antarctic origin AAIW and AABW. Moreover, this signature is transported to the Atlantic Ocean, and the slopes of the Zn-PO_4 regressions in these Antarctic origin water masses are in the same range as observed in the source regions. However, unlike the Cd-PO_4 relationship, the slope of the Zn-PO_4 relationship in SASPMW is much less steep than in AAIW and AABW. This is most likely due to the depleted concentrations of Zn in both the surface Atlantic and SASPMW source waters whereas Cd was elevated in SASPMW.

3.7. Supply From Below

Previously, it was postulated that the supply from underlying subsurface water masses is the main source of Cd and PO_4 to the surface ocean where phytoplankton grows (Middag et al., 2018). Briefly, if both elements are depleted in the surface ocean, virtually all supply is taken up, and thus, the average uptake ratio has to match the average supply ratio. Assuming all uptake is eventually remineralized as well, the average remineralization ratio also has to match the supply ratio. This in turn implies that if supply from the subsurface is the dominant supply of nutrients to the open oligotrophic ocean, a self-perpetuating cycle exists. The availability in the surface ocean is set by the supply ratio from below, and, if both elements are (nearly) quantitatively depleted and remineralized in unison, the returning exported and remineralizing particles have a ratio similar to the supply ratio. For Cd this implied a higher Cd:PO_4 supply and regional remineralization in the SH compared to the NH due to the higher ratio in Antarctic origin water masses at intermediate depth (SASPMW and AAIW; Middag et al., 2018). In the case of Zn, at greater depth Antarctic origin water masses with a high Zn/PO_4 ratios are present, but not at the deep end of the thermocline (defined as the 8 °C isotherm) due to the presence of SASPMW and NASPMW that are both very low in Zn but elevated in PO_4 (Figure 5). Although both SASPMW and NASPMW are Zn-poor, around the deep end of the thermocline, the dissolved Zn/PO_4 ratio is higher in the NH compared to the SH, as NASPMW is relatively enriched in Zn (with respect to PO_4) compared to SASPMW (Table 1). In contrast to Cd:PO_4, this would imply a lower Zn:PO_4 supply and regional remineralization ratio in the SH compared to the NH. This is in agreement with the interpretation by Wyatt et al. (2014) who also suggested the SASPMW (SAMW in Wyatt et al., 2014) brought waters that are depleted in Zn relative to PO_4. Additionally, the slope of the Zn-PO_4 relationship in the near surface is less steep in the SH compared to the NH, but no conclusions can be drawn from this as this is most likely mainly the result of mixing of different endmembers (see sections 3.3 to 3.5). Interestingly, the Zn-PO_4 relationship in the NH is with a steep slope in deep water and a gentle slope in surface waters very comparable to observations in the North Pacific Ocean (Jakuba et al., 2012; Martin et al., 1989). This indeed implies that supply depleted in Zn relative to PO_4 via SASPMW and to a lesser degree AAIW is responsible for the complex Zn-PO_4 relationship in the south Atlantic as in the absence of such water masses, qualitatively comparable Zn-PO_4 relationships are observed in very different ocean regions.

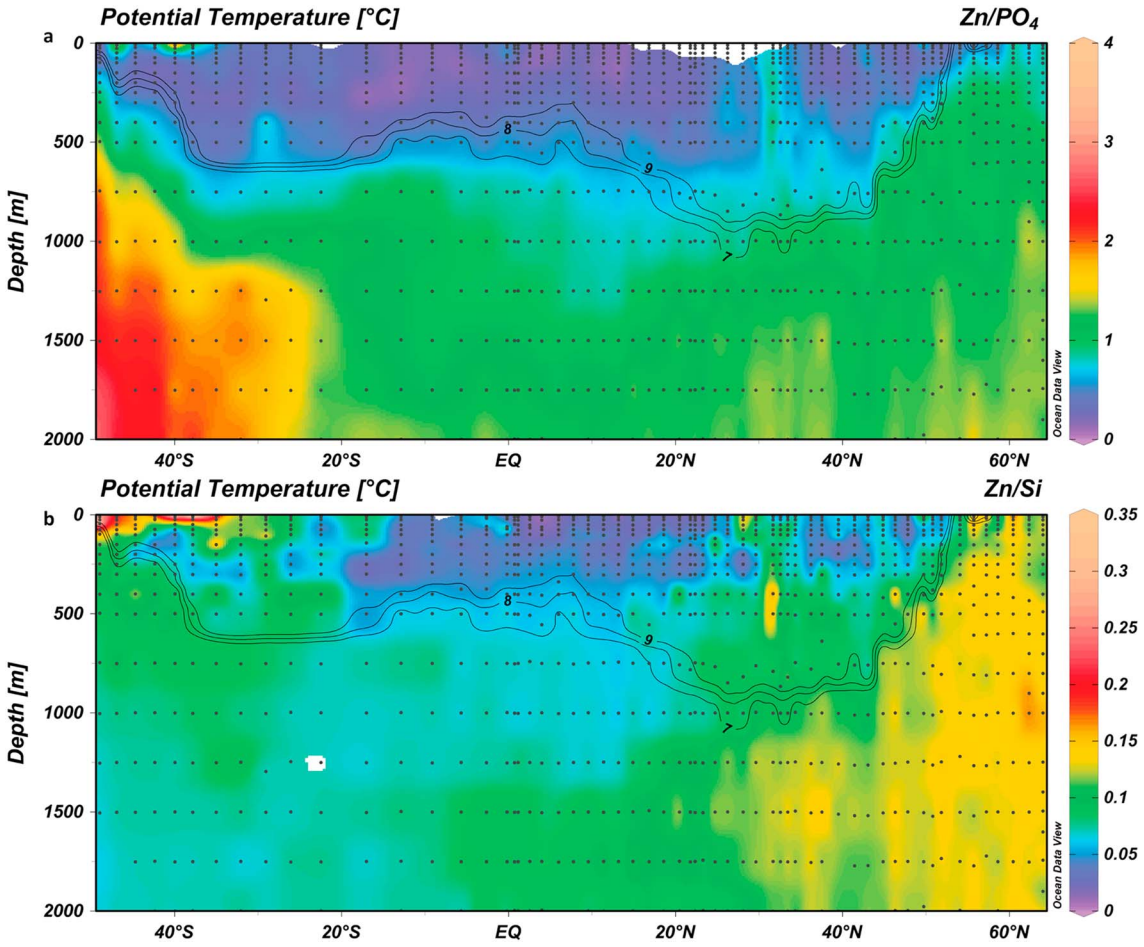

Figure 5. The dissolved Zn/nutrient ratios. (a) The Zn/PO_4 ratio. (b) The dissolved Zn/Si ratio. The ratios are in color scale with the potential temperature overlain in isobars. The location of the isobars broadly coincides with the location of the core of NASPMW in the NH and just below the core of SASPMW in the SH. Zn = zinc; NH = Northern Hemisphere; SH = Southern Hemisphere; Si = silicate; NASPMW = North Atlantic Sub-Polar Mode Water; SASPMW = South Atlantic Sub-Polar Mode Water.

3.8. Zn-Si Relationship

Akin to the Zn-PO_4 relationship, this text section will assess the Zn-Si relationship from north to south. In the far north, north of 57.5°N, there is a good correlation between Zn and Si (Figure 6a; $R^2 = 0.82$). Going southward until 50°N, low Zn and low Si (near) surface waters appear (NASPMW and NASTMW), which plot slightly below the regression line determined further north and along a regression with a steeper slope (Figure 6b). This is in contrast to the Zn-PO_4 regression, where the observed regression slope was less steep in the shallower water masses (Figure 2). Including data till 40°N, three additional features become apparent (Figure 6c). The first feature is the influence of AABW in the deep that brings waters enriched in Si, but with less Zn than would be expected based on the regression in NADW (Figure 6c), creating a kink between a Si concentration of 10 and 15 μmol/kg. Second, akin to the relationship with PO_4, there are data with a high deficit of oxygen (>100 μmol/kg), mainly around 750-m depth, that is slightly elevated in Si with respect to Zn. Third, concentrations of Zn are depleted (<0.2 nmol/kg) below Si concentrations of ~3 μmol/kg (mainly NASTMW).

For the Zn-PO_4 relationship, there was a clear kink in the NASTMW-NASPMW-NADW mixing line at low Zn (<0.5 nmol/kg), whereas in the Zn-Si relationship this kink is much more difficult to distinguish. However, the kink at the transition between NADW (DSOW) and AABW (Zn concentration ~1.5 nmol/kg) is much more noticeable in the Zn-Si relationship than in the Zn-PO_4 relationship due to the strong Si enrichment in AABW.

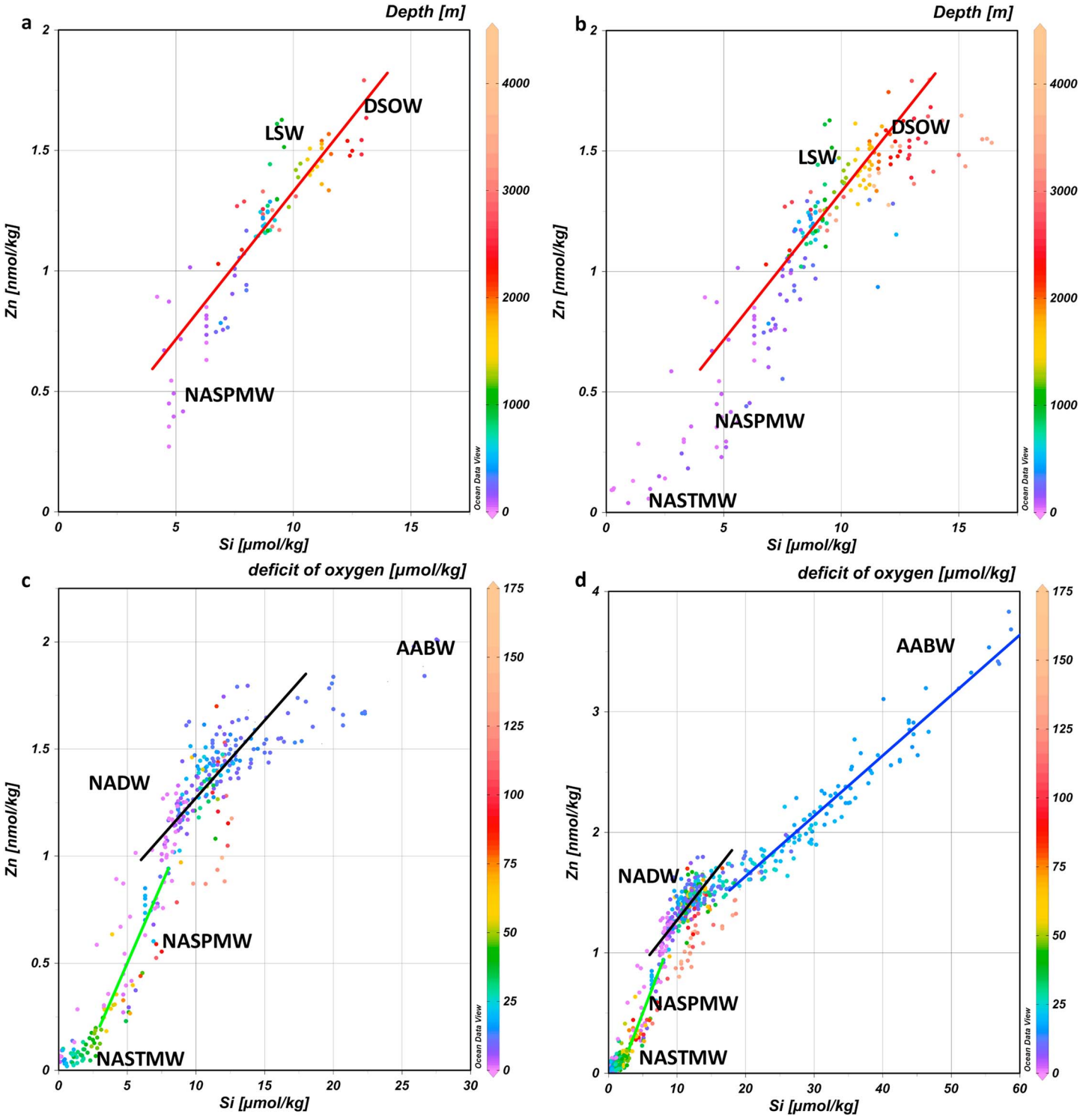

Figure 6. The Zn versus Si distribution. (a) The distribution along the transect north of 57.5°N. (b) The distribution north of 50°N. (c) The distribution north of 40°N. (d) The distribution in the entire NH. Red line is the regression in Nordic water north of 57.5°N. Green line is the regression in NASPMW mixing with NADW, the black line is the regression in NADW (NADW > 60%), and the blue line is the regression in AABW mixing with NADW north of 20°N. Color scale indicates depth in Figures 6a and 6b; color scale indicates the deficit of oxygen in Figures 6c and 6d. Equations for the regressions can be found in Table 2. Zn = zinc; Si = silicate; DSOW = Denmark Strait Overflow Water; LSW = Labrador Sea Water; NASPMW = North Atlantic Sub-Polar Mode Water; AABW = Antarctic Bottom Water; NADW = North Atlantic Deep Water.

Table 2
Regression Lines as Depicted in Figures 2, 3, 6, and 7

Regression	Equation	R^2	Data selection	n
Zn-PO_4 relationship				
Nordic water (red)	Zn = 3.0 * PO_4–1.9	0.62	>57.5°N;	$n = 92$
Northern surface (green)	Zn = 0.4 * PO_4 + 0	0.79	>50°N; Zn < 0.5;	$n = 27$
AABW NH (blue)	Zn = 4.0 * PO_4–3.1	0.82	>20°N; AABW > 0.05;	$n = 113$
AABW transect (blue)	Zn = 5.4 * PO_4–7.9	0.97	<45°S; AABW > 0.05; uCDW < 0.2;	$n = 303$
Zn-Si relationship				
Nordic water (red)	Zn = 0.14* Si – 0.03	0.82	>57.5°N;	$n = 92$
NASPMW-NADW (green)	Zn = 0.15* Si – 0.23	0.65	>40°N; Zn < 1.1, 3 < Si < 8;	$n = 69$
NADW (black)	Zn = 0.07* Si + 0.55	0.60	>40°N; NADW > 0.6; AABW < 0.05;	$n = 189$
AABW NH (blue)	Zn = 0.05* Si + 0.63	0.93	>20°N; AABW > 0.05;	$n = 113$
AABW entire transect (blue)	Zn = 0.06* Si + 0.46	0.99	AABW > 0.05; uCDW < 0.2;	$n = 352$
SACW-AAIW (gray)	Zn = 0.09* Si + 0.04	0.93	>20°S; AABW < 0.2; uCDW < 0.2; NADW < 0.2;	$n = 130$

Note. Zn = zinc; Si = silicate; PO_4 = phosphate; AABW = Antarctic Bottom Water; NH = Northern Hemisphere; uCDW = upper circumpolar deep water; NASPMW = North Atlantic Sub-Polar Mode Water; NADW = North Atlantic Deep Water; SACW = South Atlantic Central Water; AAIW = Antarctic Intermediate Water. Concentrations of Zn in nmol/kg and concentrations of Si and PO_4 in µmol/kg. Data selection for given latitude zone, for example < 45 °S is all samples northward of 45 °S; and for fraction of sample, for example AABW > 0.05 means more than 5 % AABW in the sample.

Including all samples north of 20°N, the AABW influence with high Si concentrations becomes more profound (Figure 6d). Mixing of NADW and AABW results in a kink where the slope is less steep to the right of the kink. The exact opposite was previously observed for the Cd-PO_4 relationship (Middag et al., 2018) and the Zn-PO_4 relationships where the relationship became steeper in AABW. The influence of water with an elevated deficit of oxygen becomes more profound and results in higher Si concentrations than would be expected based on the mixing between NADW and shallower water masses. This implies regional remineralization adds Zn and Si in a ratio that is lower than the slope of the Zn-Si regression in NADW-NASPMW without significant remineralization. Converting the eOMP-derived Zn:PO_4 remineralization ratio using a Si:PO_4 ratio of 15:1 results in a Zn:Si remineralization ratio of ~0.03 nmol/µmol (Table 1), which is indeed about 5 times lower than the observed slope (Table 2).

Looking at the entire NH (Figure 7a), the influence of AABW becomes stronger and another feature appears, a Zn-Si relation in the low concentration range (surface ocean) with a regression slope less steep than observed further north. This correlation can be attributed to mixing between North Atlantic surface water with South Atlantic Central Water, AAIW, and uCDW, all three influenced by regional remineralization along the section as indicated by the deficit of oxygen.

Including the SH (Figure 7b), the concentration range increases with increasing influence of AABW. As was observed in the NH and for the Zn-PO_4 distribution, the influence of regional remineralization results in a deviation from the relationships observed in the same water masses without significant influence of remineralization. This again implies regional remineralization returns Zn and Si in a Zn:Si ratio that is lower than the slope of the regression in SASPMW-AAIW without remineralization, in agreement with the eOMP-derived remineralization ratio (Table 1).

The Zn-Si relationship in the SH is quite comparable to the one in the NH (Figure 7c). In the SH, the concentrations of Zn are depleted below a Si concentration of ~3 µmol/kg and concentrations of both Zn and Si increase with increasing depth (SASPMW mixing with underlying AAIW). This results in a regression with a slope that is steeper than observed in the deep basin (AAIW mixing with underlying water masses; Figure 7c), as observed in the NH where mixing of NASPMW with NADW also resulted in a steeper slope. The Zn-Si relationship in SASPMW-AAIW plots slightly below the relationship in NASPMW-NADW in the absence of regional remineralization, and remineralization leads to deviations toward elevated Si. As was observed for the Zn/PO_4 ratio, also, the Zn/Si ratio is lower in water at the deep end of the thermocline in the NH compared to the SH, implying the supply of Zn with respect to Si from below is lower in the SH

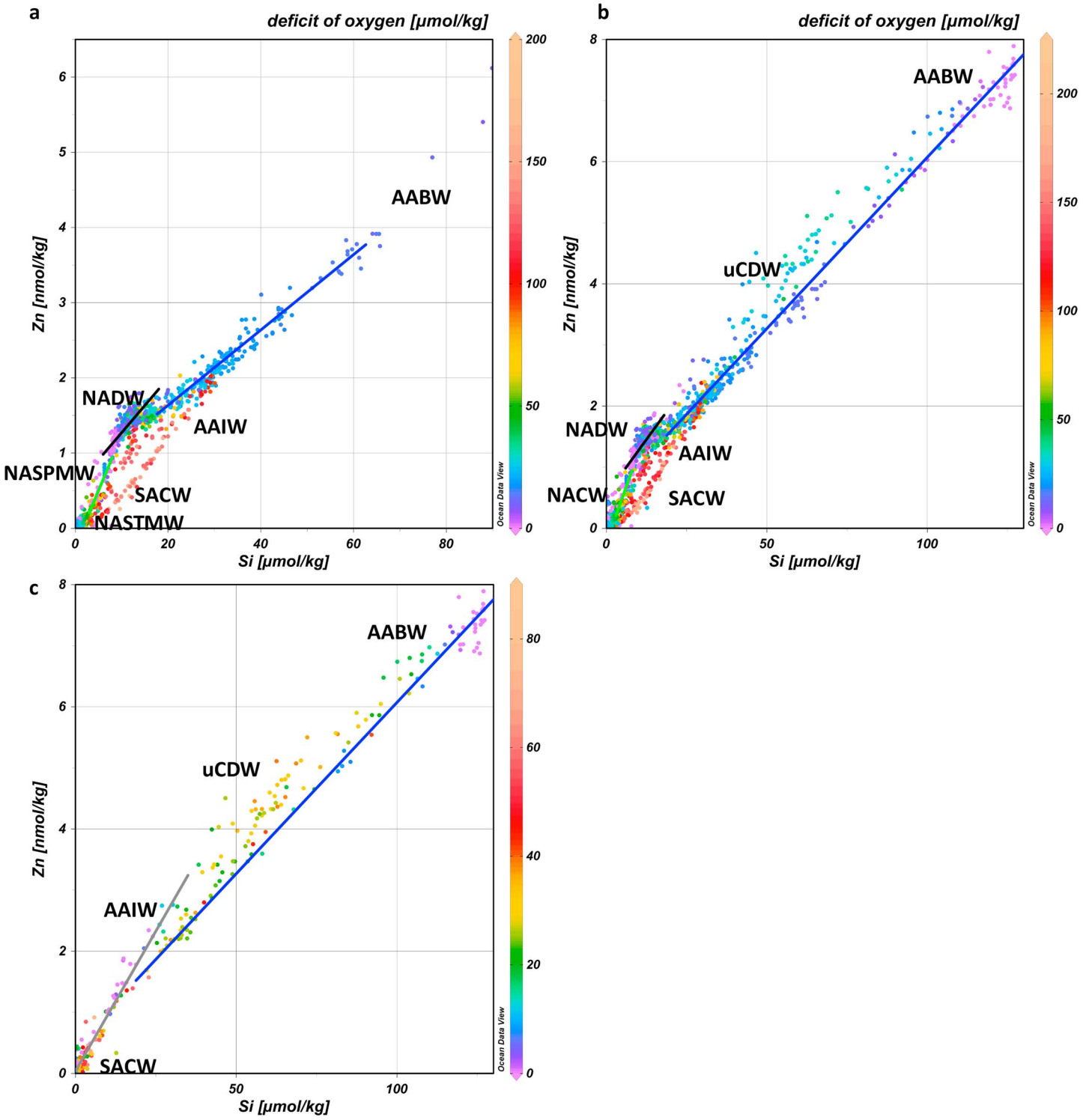

Figure 7. The Zn versus Si distribution. (a) The distribution along the transect north of the equator. (b) The distribution along the entire transect. (c) The distribution south of 20°S. Green line is the regression in NASPMW mixing with NADW (as in Figure 6), the black line is the regression in NADW (NADW > 60%; as in Figure 6), and the blue line is the regression in AABW north of 20°N in Figure 7a and along the entire transect in Figures 7b and 7c. The gray line is the regression in SACW mixing with AAIW. Color scale indicates the deficit of oxygen. Equations for the regressions can be found in Table 2. Zn = zinc; Si = silicate; AABW = Antarctic Bottom Water; NADW = North Atlantic Deep Water; uCDW = upper circumpolar deep water; AAIW = Antarctic Intermediate Water; SACW = South Atlantic Central Water; NASPMW = North Atlantic Sub-Polar Mode Water; NASTMW = North Atlantic Sub-Tropical Mode Water.

(Figure 5b). Overall, there is no general Zn-Si relationship, but the Zn-Si distribution is the result of mixing of various endmembers combined with remineralization.

Despite being an essential element and being classified as nutrient-type element, Zn does not behave like PO_4 but has a distribution more like Si as is also clearly visible in the current data set (Figure 1). Diatoms require Si as a nutrient, and they are an important class of phytoplankton that is responsible for as much as 40% of marine primary productivity (Field et al., 1998; Nelson et al., 1995), and likely even more for export production of settling particles into deep waters due to the ballast effect of the opaline diatom frustules. However, the diatoms are not dominant everywhere and are most productive in coastal, upwelling and polar regions (Armbrust, 2009, and references therein) whereas in the oligotrophic Atlantic subtropical gyres, export production and diatom productivity are relatively low (Soppa et al., 2014). All phytoplankton require Zn; thus, remineralization in regions where diatoms are not a substantial part of the phytoplankton community is mainly expected to return Zn to the dissolved phase, but not Si. In contrast, remineralization in diatom-rich regions such as the Southern Ocean and to a lesser extent the Arctic and sub-Arctic is expected to return both elements to the dissolved phase. This is visible in a relatively gentle slope of the Zn-Si relationship in NADW compared to the NH shallower water masses as well as the gentle slope in SH deeper water masses compared to the SH shallower water masses. Thus, the kink in the Zn-Si relationship at the transition between the highest latitude origin water and lower latitude origin water masses is predictable and reproduced in the eOMP model without the need to infer remineralization of Zn within the Atlantic. Similarly, the slope is less steep in AABW compared to NADW, in line with the greater nutrient drawdown by diatoms and subsequent remineralization in the Southern Ocean compared to the NADW source regions. However, the slopes of regression are not only a function of the composition of the endmembers, determined by the preformed concentrations (surface concentrations at time of formation) and the remineralization ratio in the formation region as well as during advection to the Atlantic, but also influenced by mixing during advection in the Atlantic as previously suggested (Vance et al., 2017, their Figure 3b). For example, the slope of the Zn-Si relationship in AAIW appears steeper than in AABW. However, AAIW is formed north of the APF, a region generally considered to be dominated by diatoms that strip the surface water from Si (e.g., Quéguiner et al., 1997), and thus, a gentler slope is expected. The AABW on the other hand is formed close to the Antarctic continent where diatoms often dominate, but do not deplete the Si concentrations to low concentrations. The slope of regression observed in the depth range around the core of AAIW is indeed less steep than observed in the subsurface water masses of the NH, but not as gentle as in the depth range where AABW is the dominant water mass. However, a relationship with a relatively steep slope in the surface and subsurface water masses is inherent to the mixing of these waters and the depletion of both elements in the Atlantic (near-)surface waters, whereas the underlying subsurface water AAIW is relatively elevated in Zn compared to Si. This is likely related to incomplete Zn utilization; that is, there is "left over" Zn after (near) complete Si drawdown in the source region of AAIW. This was previously observed in the formation regions of AAIW (Croot et al., 2011; Zhao et al., 2014; see also Vance et al., 2017, their Figure 3a) and also evident from the positive intercept of the Zn-Si relationship in AAIW (not shown). In contrast, AABW has high preformed concentrations (concentrations at time of formation) for both Zn and Si. During advection northward, AABW mixes with overlying CDW that also has high concentrations of both elements as generally the deep Southern Ocean is rather homogenous (see Vance et al., 2017, and references therein). This leads to a gentle slope of the Zn-Si relationship in AABW-uCDW. In fact, AABW is ultimately formed from upwelled CDW that advected southward toward the continent. As previously established (e.g., Ellwood, 2008; Vance et al., 2017; Wyatt et al., 2014), the Zn, PO_4, and Si composition of AABW as observed in the Atlantic is the resultant of the initial concentrations, uptake, remineralization, and mixing during advection. Similarly, the AAIW composition is the resultant of the same processes where notably mixing has a strong influence on the regression slope due to the different composition of the overlying (SASPMW-SASTMW) and underlying (CDW-NADW) water masses. Thus, utmost care should be taken in interpreting the slopes of the Zn-Si (or Zn-PO_4) regression lines as representative of a remineralization ratio, and the influence of mixing with different water masses of varying composition and "life history" should be taken in consideration. Nevertheless, the difference in the Zn and Si concentrations and ratios of the different endmembers (Table 1) must be (at least partly) related to different uptake and remineralization ratios in the source regions. For AABW, its endmember composition implies significant remineralization of both Si and Zn, with relatively more remineralization of Si than Zn compared to, for example, NADW. Similar to AABW, the endmember composition of AAIW has a relatively low Zn/Si ratio compared to NADW, in

line with relatively more remineralization of Si than Zn. This is consistent with greater nutrient drawdown by diatoms in the AAIW source regions than in NADW source regions.

Regional remineralization in the subsurface Atlantic Ocean has a modest effect on the Zn and Si concentrations in the subtropical gyres, but does lead to a small increase in both Zn and Si. In the equatorial region the effect of remineralization is most profound, coinciding with the highest deficits of oxygen. In the equatorial upwelling region, notably in the eastern Atlantic Ocean, diatoms flourish (Soppa et al., 2014), and hence subsequent remineralization should lead to a gentle slope of the Zn-Si relationship in the regions that are most influenced by remineralization, in accordance with our observations (Figures 6 and 7).

3.9. Differences Between the Zn-Si and the Zn-PO_4 Relationship

The most striking difference between the relationships of Zn with Si and PO_4 is the steepening of the slopes for the Zn-PO_4 relationships with influence from high-latitude origin deep water masses, whereas the slopes of the Zn-Si relationships become less steep. Additionally, the transition between NADW and AABW in the NH and the transition from AAIW to uCDW-NADW-AABW results in the largest change in slope for the Zn-Si relationship, whereas for the Zn-PO4 relationship the largest change in slope occurs at the transition between NASPMW and NADW in the NH and the transition between SASPMW and AAIW in the SH.

The steepening of the Zn-PO_4 slopes and higher endmember Zn/PO_4 ratios (Table 1) indicates higher Zn:PO_4 uptake ratios in the source regions of NADW in the north and AAIW and AABW in the south compared to Atlantic surface waters. For Cd, also a high uptake ratio was observed in SASPMW (SAMW), but not for Zn. This is consistent with previous studies that noted the depletion of Zn and Si in the more southerly formation region of AAIW, whereas Cd and PO_4 get depleted in the more northern formation region of SASPMW (e.g., Abouchami et al., 2014; Baars et al., 2014; Croot et al., 2011; Zhao et al., 2014). For the High Nutrient Low Chlorophyll (HNLC) Southern Ocean, it has been suggested that Fe limitation leads to increased uptake of other bivalent metals such as Cd and Zn, but it could also simply be related to the metal availability (e.g., Cullen, 2006; Middag et al., 2018; Sunda & Huntsman, 2000). The metal availability could be related to the total metal concentration as well as the degree of organic complexation (Baars & Croot, 2011; Croot et al., 2011). The steepening of the Zn-PO_4 relationship and higher endmember ratios in AABW compared to NADW is consistent with increased Zn uptake under either HNLC conditions or higher Zn availability. However, unlike for Cd, the uptake of Zn with respect to PO_4 in the northern source regions of NADW also appears much higher than in the Atlantic Ocean proper. This suggests the availability of Zn also plays a role in the increased Zn uptake with respect to PO_4 as the NADW source regions are not known regions of chronic Fe limitation.

Thus, the main kink in the Zn-PO_4 relationship (transition between Atlantic (near) surface water and high latitude origin water) is related to the higher Zn:PO_4 uptake ratio and subsequent higher Zn/PO_4 ratio in water masses originating from the higher latitudes. Both the NASPMW and SASPMW are depleted in Zn, but relatively elevated in PO_4 resulting in very low Zn supply from below to the lower latitude surface waters and hence a low Zn:PO_4 uptake and low remineralization ratio in the Atlantic Ocean. This leads to a relatively gentle slope in the near surface Atlantic, but a steep slope below the core of NASPMW and SASPMW due to the presence of water masses elevated in both Zn and PO_4 with a much higher Zn/PO_4 ratio. However, the NADW has lower Zn and PO_4 concentrations than overlying uCDW and AAIW and underlying AABW, leading to strong increases and decreases in concentration over the vertical water column, notably in the SH.

The main kink in the Zn-Si relationship is related to the greater productivity of diatoms at the high latitudes and the depletion of both Zn and Si in NASPMW and SASPMW. Diatom dominated productivity leads to a relatively low Zn:Si uptake and remineralization ratio compared to production by nondiatom dominated phytoplankton communities that utilize less Si. This results in a gentle slope of the Zn-Si relationship in high-latitude origin waters (notably AABW), despite the known increased bivalent metal uptake at the high latitudes. The kink occurs deeper in the water column than for the Zn-PO_4 relationship as unlike PO_4, both Zn and Si are depleted in NASPMW and SASPMW. Deeper than the depth of NASPMW and SASPMW, the Si concentration starts to increase (waters originating from relatively diatom rich regions). The mixing with the overlying NASTMW and SASTMW (depleted Si and Zn) and underlying deep water (relatively high Zn, very high Si) results in a kink. Additionally, there is an obvious kink in the

NH at the transition between NADW and AABW due to the much stronger Si increase in AABW compared to NADW. As observed for PO_4, the NADW has lower Si concentrations than underlying AABW and overlying AAIW and uCDW, leading to concentration increases and decreases over the water column. However, unlike PO_4 that is elevated to similar concentrations in the Atlantic AAIW-uCDW mixture as in AABW (in the Atlantic), Zn and Si are mainly elevated in AABW. This leads to much smaller variations in the Zn-Si relationship than observed in the Zn- PO_4 relationship, giving the appearance of a single Zn-Si regression in the deep water column, whereas in fact the data are best described by various mixing lines (see section 3.8).

3.10. Zn as a Tracer

In the Pacific Ocean, a Zn deficit with respect to Si was observed in the Oxygen Depleted Zone, which was attributed to the formation of solid Zn sulfides (Janssen & Cullen, 2015). In the Atlantic Ocean, at first glance it would appear that there is also a Zn deficit (or Si enrichment) in regions with a high deficit of oxygen (Figures 6 and 7). However, this can be explained by mixing and regional remineralization, as previously observed for Cd in the West Atlantic (Middag et al., 2018). Nevertheless, oxygen concentrations in the Atlantic are not as depleted as in the Pacific, so the absence of an actual Zn deficit in the Atlantic does not imply Zn sulfides are not formed in the Pacific. Additionally, a recent study (Weber et al., 2018) suggested Zn scavenging is not related to sulfide formation in microenvironments but occurs throughout the ocean onto organic particles and can thus occur throughout the ocean rather than specifically in Oxygen Depleted Zones. Nevertheless, the current data set does imply that the calculation of a Zn deficit or the use of a Zn* tracer should be done carefully with attention to the caveats and is unlikely to be useful over large transects or when comparing different regions due to stark contrasts in the Zn and Si composition of different water masses.

Additionally, the Zn:Ca ratio in benthic foraminifera as a paleo oceanography proxy for the Zn concentrations in deep water as indicator for the presence of southern and northern origin water (Marchitto et al., 2000; Marchitto et al., 2002) should be used with caution. For example, the used Zn:Si ratio of 0.052 (Marchitto et al., 2000) to calibrate this proxy is a very reasonable estimate of the slope of the relationship in AABW (0.056 along current transect). However, this is not the case for the slope of the relationship observed in the far north (0.14) or in NADW (0.072), leading to an underestimation of paleo-Zn in these regions. The Zn concentration in deep waters is the result of the preformed concentration and mixing during advection, combined with the effect of remineralization where the remineralization ratio probably depends on the surface Zn concentration and the degree of iron limitation in the surface ocean (HNLC conditions, see section 3.7). As the surface Zn and iron concentration will have varied over time, both the Zn concentrations of the bottom water masses and the remineralization ratio will have varied. This in turn has consequences for the calculations of the relative contributions of northern and southern origin water masses. Thus, we recommend not to use a fixed Zn:Si or Zn:PO_4 remineralization ratio (also not recommended for the Cd:PO_4 ratio; Middag et al., 2018). Instead, we think it is prudent to include an estimate of variability of these ratios and to acknowledge the remineralization ratio is likely different between different regions (notably high latitude northern and southern origin water masses) and thus should not be based on the overall regression in global data compilations or without regard for the influence of water mass mixing. Notably, regressions based on global data compilations are inherently biased toward southern origin water masses due to the absence of deep water of northern origin outside the Atlantic and the greater nutrient depletion in the Southern Ocean.

The Zn:Si ratios derived from the slopes of regression reported in this and previous studies on dissolved Zn in the water column (e.g., Bruland, 1980; Croot et al., 2011; Janssen & Cullen, 2015; Wyatt et al., 2014) are one to two orders of magnitude higher than observed in diatom frustules in sediment cores (Ellwood & Hunter, 2000b; Hendry & Rickaby, 2008). This confirms the majority of Zn taken up by diatoms is not present in the frustule, but in the organic parts of the cell. Changes in Zn uptake into the organic parts of the cell are not necessarily represented in the Zn:Si ratio of the diatom frustules, as it is currently uncertain what drives Zn incorporation into siliceous frustules. Further research is needed to unravel the potential coupling between the Zn:Si ratio in diatom frustules and the Zn availability and uptake in the surface ocean in order to assess the use of this proxy.

4. Conclusions

The assessment of the distributions of Zn, Si, and PO_4 along the GEOTRACES GA03 West-Atlantic transect reveals there is no general Zn-Si or Zn-PO_4 relationship that can be accurately described by a single or bilinear regression. The Zn distribution is governed by mixing of the various water masses along this transect where regional remineralization (i.e., within the Atlantic) has a significant influence on the PO_4 distribution, but not on the Zn and Si distribution. The maximum observed deficit of oxygen of ~200 μmol/kg due to remineralization along the section, implies a maximum remineralization of PO_4, Si and Zn of ~1.2 μmol/kg, 5.9 μmol/kg, and 0.5 nmol/kg, respectively. Given the maximum observed concentrations of 2.4 μmol/kg, 127 μmol/kg, and 8 nmol/kg, for PO_4, Si, and Zn, respectively, it is not surprising the effects of remineralization are much more difficult to distinguish from mixing for Si and Zn than for PO_4 (or Cd). The highest observed concentrations for all three are associated with the deep waters from the Antarctic region. Thus, it is confirmed that the high latitudes play a crucial role in the distribution of major and trace nutrients in the Atlantic Ocean as previously suggested (e.g., Ellwood, 2008; Middag et al., 2018; Saito et al., 2010; Sarmiento et al., 2004; Sunda & Huntsman, 2000; Vance et al., 2017 ; Wyatt et al., 2014). Thus far, mainly the influence of the Antarctic region has been emphasized, which indeed is a dominant driver due to the larger drawdown and subsequent return of nutrients in deep water. However, the northern high latitudes and source region of NASPMW and NADW should not be overlooked. Notably in the Atlantic, the mixing between NADW and AABW is a key driver for the observed distribution of nutrients and trace elements. Additionally, NASPMW is relatively depleted in Zn and thus plays a role in the very limited supply of Zn to the surface Atlantic Ocean.

From the Antarctic origin water masses, AABW plays an important role, as it brings in high concentrations of Zn, Si, and PO_4. The AAIW on the other hand is largely depleted in Si but has some "left over Zn" and high PO_4, whereas SASPWM formed further north is depleted in Zn, Si, and PO_4. This indeed leads to a very low supply into surface waters from below for Zn and Si compared to PO_4 as previously suggested (Vance et al., 2017; Wyatt et al., 2014). The very low concentrations of Zn and Si in the SH surface and near surface waters, including SASPMW, whereas the underlying AAIW is slightly elevated in Zn but not as much in Si, lead to a Zn-Si correlation with a steep slope. The latter is mainly the result of mixing of these water masses rather than a regional remineralization signature; that is, this slope of regression is a good example were the slope derived Zn:Si ratio is not representative of a remineralization ratio. Scavenging of Zn as postulated previously (John & Conway, 2014; Weber et al., 2018) may play a role in explaining the very gentle Zn:PO_4 slope in the upper surface (or lack of a relationship). However, the very limited supply of Zn from underlying water which is more depleted in Zn than Si also explains the Zn distribution and the eOMP modeled Zn concentrations match the observations very well, that is, without a need to invoke an additional mechanism such as scavenging. Nevertheless, we cannot exclude scavenging, as obviously, there is still some discrepancy between the modeled concentrations and the observations.

For the Zn-PO_4 relationship, the most profound kink is caused by a higher Zn:PO_4 uptake and remineralization ratio in high latitude waters. This is the case for both Nordic and Antarctic origin waters, implying a driving role of Zn availability rather than Fe limitation unless the NADW source regions are HNLC regions that may be subject to (seasonal) Fe limitation. However, a second, less profound, kink is observed in the Zn-PO_4 HNLC relationship between AABW and NADW. This implies a higher uptake and remineralization ratio in the far south, suggesting that increased Zn uptake under HNLC conditions could be a factor on top of the availability driven uptake. Alternatively, the phytoplankton community composition rather than Fe and/or Zn availability could influence the Zn:PO_4 uptake and remineralization ratio in high-latitude oceans.

Overall, the distribution of Zn is mainly the result of mixing of various water masses where both the Nordic and Antarctic origin water masses play an important role. Both the NASPWM and the SASPMW are depleted in Zn with respect to the deeper water masses, implying the depletion of Zn occurs not only in the source region of SASPMW (SAMW) as previously suggested (Vance et al., 2017; Wyatt et al., 2014), but also in the source region of NASPMW. As these water masses form an important supply of nutrients to the surface waters of the Atlantic, this supply from below of Zn is very small. It appears the supply from below of Zn is lower in the SH compared to the NH, in contrast to the major nutrients and trace metal Cd. This leads to very low Zn concentration in the surface ocean throughout the Atlantic Ocean, explaining why

regional remineralization of Zn plays a very small role in the Zn distribution of the Atlantic. Additionally, the surface concentrations of Cd (Middag et al., 2018) and Co (Dulaquais et al., 2014) are also very low in the Atlantic surface waters. This implies the availability of these metals might influence community composition and primary productivity in the West-Atlantic, as different species have different requirements and efficiencies and Zn, Cd, and Co can partially replace each other depending on the species (e.g., Morel et al., 2014; Saito et al., 2002). Further targeted research will be required to determine the effects of the very low concentrations of Zn, Co, and Cd on phytoplankton in the Atlantic Ocean and how sensitive the distribution of these elements is to changes in the high-latitude oceans.

Acknowledgments

We express our gratitude to the captains and crew of the RV Pelagia and RRS James Cook during the cruises. The nutrient data were provided by the NIOZ nutrient lab and the oxygen data by Lesley Salt and Maaike Claus. Steven van Heuven provided advice on the eOMP modeling and helped adapting the code to work for Zn. This work was supported by the Netherlands Organization for Scientific Research (NWO) project Grants 820.01.014 (GEOTRACES Netherlands-USA Joint Effort on Trace Metals in the Atlantic Ocean; post-doc of R. M. at UCSC) and 839.08.410 (GEOTRACES, Global Change and Microbial Oceanography in the West Atlantic Ocean) and the USA National Science Foundation (NSF) Grant OCE-0961579. All data reported in this paper are available through the GEOTRACES data repository (http://geotraces.org/dp/idp2017) at the British Oceanographic Data Centre as detailed by Schlitzer et al. (2018). Figures were made using ODV (Schlitzer, 2016). H. d. B. designed the GA02 section, organized the expeditions and funding for the cruise program and construction of PVDF samplers. R. M. with colleagues of the NIOZ trace metals group did all the sampling and filtrations during the four cruises. R. M. and K. B. further developed the method of Biller and Bruland (2012) and did all the analyses of Zn and several other trace metals in 1,433 samples at UCSC. R. M. did the eOMP analysis and produced the manuscript. The authors are grateful to the two reviewers for their positive comments and constructive suggestions.

References

Abouchami, W., Galer, S. J. G., de Baar, H. J. W., Middag, R., Vance, D., Zhao, Y., et al. (2014). Biogeochemical cycling of cadmium isotopes in the Southern Ocean along the Zero Meridian. *Geochimica et Cosmochimica Acta*, *127*, 348–367. https://doi.org/10.1016/j.gca.2013.10.022

Armbrust, E. V. (2009). The life of diatoms in the world's oceans. *Nature*, *459*(7244), 185–192. https://doi.org/10.1038/nature08057

Baars, O., Abouchami, W., Galer, S. J. G., Boye, M., & Croot, P. L. (2014). Dissolved cadmium in the Southern Ocean: Distribution, speciation, and relation to phosphate. *Limnology and Oceanography*, *59*(2), 385–399. https://doi.org/10.4319/lo.2014.59.2.0385

Baars, O., & Croot, P. L. (2011). The speciation of dissolved zinc in the Atlantic sector of the Southern Ocean. *Deep Sea Research Part II: Topical Studies in Oceanography*, *58*(25-26), 2720–2732. https://doi.org/10.1016/j.dsr2.2011.02.003

Biller, D. V., & Bruland, K. W. (2012). Analysis of Mn, Fe, Co, Ni, Cu, Zn, Cd, and Pb in seawater using the Nobias-chelate PA1 resin and magnetic sector inductively coupled plasma mass spectrometry (ICP-MS). *Marine Chemistry*, *130–131*, 12–20. https://doi.org/10.1016/j.marchem.2011.12.001

Broecker, W. S. (1991). The great ocean conveyor. *Oceanography*, *4*(2), 79–89. https://doi.org/10.5670/oceanog.1991.07

Bruland, K. W. (1980). Oceanographic distributions of cadmium, zinc, nickel, and copper in the North Pacific. *Earth and Planetary Science Letters*, *47*(2), 176–198. https://doi.org/10.1016/0012-821X(80)90035-7

Bruland, K. W., Donat, J. R., & Hutchins, D. A. (1991). Interactive influences of bioactive trace-metals on biological production in oceanic waters. *Limnology and Oceanography*, *36*(8), 1555–1577. https://doi.org/10.4319/lo.1991.36.8.1555

Bruland, K. W., Franks, R. P., Knauer, G. A., & Martin, J. H. (1979). Sampling and analytical methods for the determination of copper, cadmium, zinc, and nickel at the nanogram per liter level in sea-water. *Analytica Chimica Acta*, *105*(1), 233–245. https://doi.org/10.1016/S0003-2670(01)83754-5

Bruland, K. W., Middag, R., & Lohan, M. C. (2014). 8.2—Controls of trace metals in seawater A2 - Holland, Heinrich D. In K. K. Turekian (Ed.), *Treatise on geochemistry*, (Second ed.pp. 19–51). Oxford: Elsevier. https://doi.org/10.1016/B978-0-08-095975-7.00602-1

Conway, T. M., & John, S. G. (2014). The biogeochemical cycling of zinc and zinc isotopes in the North Atlantic Ocean. *Global Biogeochemical Cycles*, *28*, 1111–1128. https://doi.org/10.1002/2014GB004862

Croot, P. L., Baars, O., & Streu, P. (2011). The distribution of dissolved zinc in the Atlantic sector of the Southern Ocean. *Deep Sea Research Part II: Topical Studies in Oceanography*, *58*(25-26), 2707–2719. https://doi.org/10.1016/j.dsr2.2010.10.041

Cullen, J. T. (2006). On the nonlinear relationship between dissolved cadmium and phosphate in the modern global ocean: Could chronic iron limitation of phytoplankton growth cause the kink? *Limnology and Oceanography*, *51*(3), 1369–1380. https://doi.org/10.4319/lo.2006.51.3.1369

Danielsson, L.-G., & Westerlund, S. (1983). Trace metals in the Arctic Ocean. In C. S. Wong, E. Boyle, K. W. Bruland, J. D. Burton, & E. D. Goldberg (Eds.), *Trace metals in sea water*, (pp. 85–95). Boston, MA: Springer US. https://doi.org/10.1007/978-1-4757-6864-0_5

de Baar, H. J. W., Timmermans, K. R., Laan, P., De Porto, H. H., Ober, S., Blom, J. J., et al. (2008). Titan: A new facility for ultraclean sampling of trace elements and isotopes in the deep oceans in the international Geotraces program. *Marine Chemistry*, *111*(1–2), 4–21. https://doi.org/10.1016/j.marchem.2007.07.009

de Baar, H. J. W., van Heuven, S. M. A. C., & Middag, R. (2018). Ocean biochemical cycling and trace elements. In W. M. White (Ed.), *Encyclopedia of geochemistry: A comprehensive reference source on the chemistry of the Earth*, (pp. 1–21). Cham: Springer International Publishing.

Dulaquais, G., Boye, M., Middag, R., Owens, S., Puigcorbe, V., Buesseler, K., et al. (2014). Contrasting biogeochemical cycles of cobalt in the surface western Atlantic Ocean. *Global Biogeochemical Cycles*, *28*, 1387–1412. https://doi.org/10.1002/2014GB004903

Ellwood, M. J. (2008). Wintertime trace metal (Zn, Cu, Ni, Cd, Pb and Co) and nutrient distributions in the Subantarctic Zone between 40-52 degrees S; 155-160 degrees E. *Marine Chemistry*, *112*(1–2), 107–117. https://doi.org/10.1016/j.marchem.2008.07.008

Ellwood, M. J., & Hunter, K. A. (2000a). The incorporation of zinc and iron into the frustule of the marine diatom Thalassiosira pseudonana. *Limnology and Oceanography*, *45*(7), 1517–1524. https://doi.org/10.4319/lo.2000.45.7.1517

Ellwood, M. J., & Hunter, K. J. (2000b). Variations in the Zn/Si record over the Last Interglacial Glacial Transition. *Paleoceanography*, *15*, 506–514. https://doi.org/10.1029/1999PA000470

Field, C. B., Behrenfeld, M. J., Randerson, J. T., & Falkowski, P. (1998). Primary production of the biosphere: Integrating terrestrial and oceanic components. *Science*, *281*(5374), 237–240. https://doi.org/10.1126/science.281.5374.237

Grashoff, K., Ehrhardt, M., & Kremling, K. (1983). Methods of Seawater Analysis. Verlag Chemie, Weinheim, Germany.

Hendry, K. R., & Rickaby, R. E. M. (2008). Opal (Zn/Si) ratios as a nearshore geochemical proxy in coastal Antarctica. *Paleoceanography*, *23*, PA2218. https://doi.org/10.1029/2007PA001576

Ho, T. Y., Quigg, A., Finkel, Z. V., Milligan, A. J., Wyman, K., Falkowski, P. G., & Morel, F. M. M. (2003). The elemental composition of some marine phytoplankton. *Journal of Phycology*, *39*(6), 1145–1159. https://doi.org/10.1111/j.0022-3646.2003.03-090.x

Jakuba, R. W., Moffett, J. W., & Dyhrman, S. T. (2008). Evidence for the linked biogeochemical cycling of zinc, cobalt, and phosphorus in the western North Atlantic Ocean. *Global Biogeochemical Cycles*, *22*, GB4012. https://doi.org/10.1029/2007GB003119

Jakuba, R. W., Saito, M. A., Moffett, J. W., & Xu, Y. (2012). Dissolved zinc in the subarctic North Pacific and Bering Sea: Its distribution, speciation, and importance to primary producers. *Global Biogeochemical Cycles*, *26*, GB2015. https://doi.org/10.1029/2010GB004004

Janssen, D. J., & Cullen, J. T. (2015). Decoupling of zinc and silicic acid in the subarctic Northeast Pacific interior. *Marine Chemistry*, *177*(part 1), 124–133. https://doi.org/10.1016/j.marchem.2015.03.014

John, S. G., & Conway, T. M. (2014). A role for scavenging in the marine biogeochemical cycling of zinc and zinc isotopes. *Earth and Planetary Science Letters*, *394*(supplement C), 159–167. https://doi.org/10.1016/j.epsl.2014.02.053

Karstensen, J., & Tomczak, M. (1998). Age determination of mixed water masses using CFC and oxygen data. *Journal of Geophysical Research*, *103*, 18,599–18,609. https://doi.org/10.1029/98JC00889

Kim, T., Obata, H., Nishioka, J., & Gamo, T. (2017). Distribution of dissolved zinc in the western and central subarctic North Pacific. *Global Biogeochemical Cycles*, *31*, 1454–1468. https://doi.org/10.1002/2017GB005711

Klunder, M. B., Laan, P., Middag, R., de Baar, H. J. W., & van Ooijen, J. C. (2011). Dissolved iron in the Southern Ocean (Atlantic sector). *Deep-Sea Research Part II-Topical Studies in Oceanography*, *58*(25–26), 2678–2694. https://doi.org/10.1016/j.dsr2.2010.10.042

Lancelot, C., Hannon, E., Becquevort, S., Veth, C., & de Baar, H. J. W. (2000). Modeling phytoplankton blooms and carbon export production in the Southern Ocean: Dominant controls by light and iron in the Atlantic sector in Austral spring 1992. *Deep Sea Research Part I: Oceanographic Research Papers*, *47*(9), 1621–1662. https://doi.org/10.1016/S0967-0637(00)00005-4

Little, S. H., Vance, D., McManus, J., & Severmann, S. (2016). Key role of continental margin sediments in the oceanic mass balance of Zn and Zn isotopes. *Geology*, *44*(3), 207–210. https://doi.org/10.1130/G37493.1

Lohan, M. C., Statham, P. J., & Crawford, D. W. (2002). Total dissolved zinc in the upper water column of the subarctic North East Pacific. *Deep Sea Research Part II: Topical Studies in Oceanography*, *49*(24-25), 5793–5808. https://doi.org/10.1016/S0967-0645(02)00215-1

Mackas, D. L., Denman, K. L., & Bennett, A. F. (1987). Least squares multiple tracer analysis of water mass composition. *Journal of Geophysical Research*, *92*, 2907–2918. https://doi.org/10.1029/JC092iC03p02907

Marchitto, T. M., Curry, W. B., & Oppo, D. W. (2000). Zinc concentrations in benthic foraminifera reflect seawater chemistry. *Paleoceanography*, *15*, 299–306. https://doi.org/10.1029/1999PA000420

Marchitto, T. M., Oppo, D. W., & Curry, W. B. (2002). Paired benthic foraminiferal Cd/Ca and Zn/Ca evidence for a greatly increased presence of Southern Ocean Water in the glacial North Atlantic. *Paleoceanography*, *17*(3), 1038. https://doi.org/10.1029/2000PA000598

Martin, J. H., Gordon, R. M., Fitzwater, S., & Broenkow, W. W. (1989). Vertex: Phytoplankton/iron studies in the Gulf of Alaska. *Deep Sea Research Part A. Oceanographic Research Papers*, *36*(5), 649–680. https://doi.org/10.1016/0198-0149(89)90144-1

Mawji, E., Schlitzer, R., Dodas, E. M., Abadie, C., Abouchami, W., Anderson, R. F., et al. (2015). The GEOTRACES intermediate data product 2014. *Marine Chemistry*, *177*(Part 1), 1–8. https://doi.org/10.1016/j.marchem.2015.04.005

Middag, R., de Baar, H. J. W., Laan, P., Cai, P. H., & van Ooijen, J. C. (2011). Dissolved manganese in the Atlantic sector of the Southern Ocean. *Deep-Sea Research Part II-Topical Studies in Oceanography*, *58*(25–26), 2661–2677. https://doi.org/10.1016/j.dsr2.2010.10.043

Middag, R., Séférian, R., Conway, T. M., John, S. G., Bruland, K. W., & de Baar, H. J. W. (2015). Intercomparison of dissolved trace elements at the Bermuda Atlantic time series station. *Marine Chemistry*, *177*(Part 3), 476–489. https://doi.org/10.1016/j.marchem.2015.06.014

Middag, R., van Heuven, S. M. A. C., Bruland, K. W., & de Baar, H. J. W. (2018). The relationship between cadmium and phosphate in the Atlantic Ocean unravelled. *Earth and Planetary Science Letters*, *492*, 79–88. https://doi.org/10.1016/j.epsl.2018.03.046

Middag, R., van Hulten, M. M. P., van Aken, H. M., Rijkenberg, M. J. A., Gerringa, L. J. A., Laan, P., & de Baar, H. J. W. (2015). Dissolved aluminium in the ocean conveyor of the West Atlantic Ocean: Effects of the biological cycle, scavenging, sediment resuspension and hydrography. *Marine Chemistry*, *177*(Part 1), 69–86. https://doi.org/10.1016/j.marchem.2015.02.015

Moore, R. M. (1981). Oceanographic distributions of zinc, cadmium, copper and aluminium in waters of the central arctic. *Geochimica et Cosmochimica Acta*, *45*(12), 2475–2482.

Morel, F. M. M., Cox, E. H., Kraepiel, A. M. L., Lane, T. W., Milligan, A. J., Schaperdoth, I., et al. (2002). Acquisition of inorganic carbon by the marine diatom Thalassiosira weissflogii. *Functional Plant Biology*, *29*(3), 301–308. https://doi.org/10.1071/pp01199

Morel, F. M. M., Milligan, A. J., & Saito, M. A. (2014). 8.5—Marine bioinorganic chemistry: The role of trace metals in the oceanic cycles of major nutrients. In H. D. Holland, & K. K. Turekian (Eds.), *Treatise on geochemistry*, (Second ed.pp. 123–150). Oxford: Elsevier. https://doi.org/10.1016/B978-0-08-095975-7.00605-7

Morel, F. M. M., Reinfelder, J. R., Roberts, S. B., Chamberlain, C. P., Lee, J. G., & Yee, D. (1994). Zinc and carbon co-limitation of marine phytoplankton. *Nature*, *369*(6483), 740–742. https://doi.org/10.1038/369740a0

Nelson, D. M., Tréguer, P., Brzezinski, M. A., Leynaert, A., & Quéguiner, B. (1995). Production and dissolution of biogenic silica in the ocean: Revised global estimates, comparison with regional data and relationship to biogenic sedimentation. *Global Biogeochemical Cycles*, *9*, 359–372. https://doi.org/10.1029/95GB01070

Provost, C., Escoffier, C., Maamaatuaiahutapu, K., Kartavtseff, A., & Garcon, V. (1999). Subtropical mode waters in the South Atlantic Ocean. *Journal of Geophysical Research*, *104*, 21,033–21,049. https://doi.org/10.1029/1999JC900049

Quéguiner, B., Tréguer, P., Peeken, I., & Scharek, R. (1997). Biogeochemical dynamics and the silicon cycle in the Atlantic sector of the Southern Ocean during austral spring 1992. *Deep Sea Research Part II: Topical Studies in Oceanography*, *44*(1-2), 69–89. https://doi.org/10.1016/S0967-0645(96)00066-5

Rijkenberg, M. J. A., de Baar, H. J. W., Bakker, K., Gerringa, L. J. A., Keijzer, E., Laan, M., et al. (2015). "PRISTINE", a new high volume sampler for ultraclean sampling of trace metals and isotopes. *Marine Chemistry*, *177*(Part 3), 501–509. https://doi.org/10.1016/j.marchem.2015.07.001

Rijkenberg, M. J. A., Middag, R., Laan, P., Gerringa, L. J. A., van Aken, H. M., Schoemann, V., et al. (2014). The distribution of dissolved Iron in the West Atlantic Ocean. *PLoS One*, *9*(6). https://doi.org/10.1371/journal.pone.0101323

Roshan, S., & Wu, J. (2015). Water mass mixing: The dominant control on the zinc distribution in the North Atlantic Ocean. *Global Biogeochemical Cycles*, *29*, 1060–1074. https://doi.org/10.1002/2014GB005026

Saito, M. A., Goepfert, T. J., Noble, A. E., Bertrand, E. M., Sedwick, P. N., & Ditullio, G. R. (2010). A seasonal study of dissolved cobalt in the Ross Sea, Antarctica: Micronutrient behavior, absence of scavenging, and relationships with Zn, Cd, and P. *Biogeosciences*, *7*(12), 4059–4082. https://doi.org/10.5194/bg-7-4059-2010

Saito, M. A., Moffett, J. W., Chisholm, S. W., & Waterbury, J. B. (2002). Cobalt limitation and uptake in Prochlorococcus. *Limnology and Oceanography*, *47*(6), 1629–1636. https://doi.org/10.4319/lo.2002.47.6.1629

Sarmiento, J. L., Gruber, N., Brzezinski, M. A., & Dunne, J. P. (2004). High-latitude controls of thermocline nutrients and low latitude biological productivity. *Nature*, *427*(6969), 56–60. https://doi.org/10.1038/nature02127

Schlitzer, R. (2016). Ocean Data View, https://odv.awi.de

Schlitzer, R., Anderson, R. F., Dodas, E. M., Lohan, M., Geibert, W., Tagliabue, A., et al. (2018). The GEOTRACES intermediate data product 2017. *Chemical Geology*, *493*, 210–223. https://doi.org/10.1016/j.chemgeo.2018.05.040

Shaked, Y., Xu, Y., Leblanc, K., & Morel, F. M. M. (2006). Zinc availability and alkaline phosphatase activity in Emiliania huxleyi: Implications for Zn-P co-limitation in the ocean. *Limnology and Oceanography*, *51*(1), 299–309. https://doi.org/10.4319/lo.2006.51.1.0299

Sohrin, Y., & Bruland, K. W. (2011). Global status of trace elements in the ocean. *TrAC Trends in Analytical Chemistry*, *30*(8), 1291–1307. https://doi.org/10.1016/j.trac.2011.03.006

Soppa, M., Hirata, T., Silva, B., Dinter, T., Peeken, I., Wiegmann, S., & Bracher, A. (2014). Global retrieval of diatom abundance based on phytoplankton pigments and satellite data. *Remote Sensing*, *6*(10), 10,089–10,106. https://doi.org/10.3390/rs61010089

Stramma, L., & England, M. H. (1999). On the water masses and mean circulation of the South Atlantic Ocean. *Journal of Geophysical Research*, *104*, 20,863–20,883. https://doi.org/10.1029/1999JC900139

Sunda, W. G., & Huntsman, S. A. (2000). Effect of Zn, Mn, and Fe on Cd accumulation in phytoplankton: Implications for oceanic Cd cycling. *Limnology and Oceanography*, *45*(7), 1501–1516. https://doi.org/10.4319/lo.2000.45.7.1501

Taylor, S. R. (1964). Abundance of chemical elements in the continental crust: A new table. *Geochimica et Cosmochimica Acta*, *28*(8), 1273–1285. https://doi.org/10.1016/0016-7037(64)90129-2

Tomczak, M. (1981). A multi-parameter extension of temperature/salinity diagram techniques for the analysis of non-isopycnal mixing. *Progress in Oceanography*, *10*(3), 147–171. https://doi.org/10.1016/0079-6611(81)90010-0

Twining, B. S., & Baines, S. B. (2013). The trace metal composition of marine phytoplankton. *Annual Review of Marine Science*, *5*(1), 191–215. https://doi.org/10.1146/annurev-marine-121211-172322

Twining, B. S., Baines, S. B., Bozard, J. B., Vogt, S., Walker, E. A., & Nelson, D. M. (2011). Metal quotas of plankton in the equatorial Pacific Ocean. *Deep Sea Research Part II: Topical Studies in Oceanography*, *58*(3-4), 325–341. https://doi.org/10.1016/j.dsr2.2010.08.018

Twining, B. S., Baines, S. B., & Fisher, N. S. (2004a). Element stoichiometries of individual plankton cells collected during the Southern Ocean Iron experiment (SOFeX). *Limnology and Oceanography*, *49*(6), 2115–2128. https://doi.org/10.4319/lo.2004.49.6.2115

Twining, B. S., Baines, S. B., & Fisher, N. S. (2004b). Metal cycling through plankton communities: A single-cell approach using synchroton-based x-ray fluorescence. *Rapport du Congress de la CIESM*, *37*, 251–251.

van Aken, H. M. (2007). *The oceanic thermohaline circulation: An introduction*. New York, USA: Springer Science + Business Media. https://doi.org/10.1007/978-0-387-48039-8

van Hulten, M., Middag, R., Dutay, J. C., de Baar, H. J. W., Roy-Barman, M., Gehlen, M., et al. (2017). Manganese in the West Atlantic Ocean in the context of the first global ocean circulation model of manganese. *Biogeosciences*, *14*(5), 1123–1152. https://doi.org/10.5194/bg-14-1123-2017

van Hulten, M. M. P., Sterl, A., Middag, R., de Baar, H. J. W., Gehlen, M., Dutay, J. C., & Tagliabue, A. (2014). On the effects of circulation, sediment resuspension and biological incorporation by diatoms in an ocean model of aluminium. *Biogeosciences*, *11*(14), 3757–3779. https://doi.org/10.5194/bg-11-3757-2014

van Hulten, M. M. P., Sterl, A., Tagliabue, A., Dutay, J. C., Gehlen, M., de Baar, H. J. W., & Middag, R. (2013). Aluminium in an ocean general circulation model compared with the West Atlantic Geotraces cruises. *Journal of Marine Systems*, *126*, 3–23. https://doi.org/10.1016/j.jmarsys.2012.05.005

Vance, D., Little, S. H., de Souza, G. F., Khatiwala, S., Lohan, M. C., & Middag, R. (2017). Silicon and zinc biogeochemical cycles coupled through the Southern Ocean. *Nature Geoscience*, *10*(3), 202–206. https://doi.org/10.1038/ngeo2890

Weber, T., John, S., Tagliabue, A., & DeVries, T. (2018). Biological uptake and reversible scavenging of zinc in the global ocean. *Science*, *361*(6397), 72–76. https://doi.org/10.1126/science.aap8532

Wyatt, N. J., Milne, A., Woodward, E. M. S., Rees, A. P., Browning, T. J., Bouman, H. A., et al. (2014). Biogeochemical cycling of dissolved zinc along the GEOTRACES South Atlantic transect GA10 at 40°S. *Global Biogeochemical Cycles*, *28*, 44–56. https://doi.org/10.1002/2013GB004637

Zhao, Y., Vance, D., Abouchami, W., & de Baar, H. J. W. (2014). Biogeochemical cycling of zinc and its isotopes in the Southern Ocean. *Geochimica et Cosmochimica Acta*, *125*(Supplement C), 653–672. https://doi.org/10.1016/j.gca.2013.07.045